

Acta technologica agriculturae 4
Nitra, Slovaca Universitas Agriculturae Nitriae, 2011, s. 85–89

CALCULATION OF DIFFERENT MODELS OF ARCH STRUCTURE MADE OF PVC TUBES VÝPOČET RÔZNYCH MODELOV OBLÚKOVEJ KONŠTRUKCIE Z PVC RÚROK

Dušan PÁLEŠ, Milada BALKOVÁ

Slovak University of Agriculture in Nitra, Slovak Republic

The paper deals with the computation of stresses from self-weight load of roof arch structure made of polyvinylchloride (PVC) tubes. We formed a conceptual model of this structure (Priecel a Páleš, 2008). After definition of entire geometry we computed the value of self-weight load induced by the tubes and covering sheet. The model was mathematically simulated using different edge conditions: as a three-joint arch (Páleš a Priecel, 2009), as a two-joint arch (Páleš a Balková, 2011 a) and as a double fixed arch (Páleš a Balková, 2011 b). For all these conditions we designed individual algorithms of computation to determine the resulting stresses in the PVC tubes and in their joints caused by the load. Resulting from the stress values we made efforts to assess an optimal way of structure fitting to the floor by means of a laboratory measurement. According to the obtained results, the two-joint arch is considered as the best model. Less favourable was the double fixed arch and the most unfavourable was the three-joint arch. This paper summarises the actual partial results which were presented at the scientific conferences.

Key words: structure from polyvinylchloride tubes, three-joint arch, two-joint arch, double fixed arch, self-weight load

In the paper (Priecel and Páleš, 2008), we designed a laboratory model of an arch structure created by the polyvinylchloride (PVC) tubes. Its basic dimensions are presented in Figure 1.

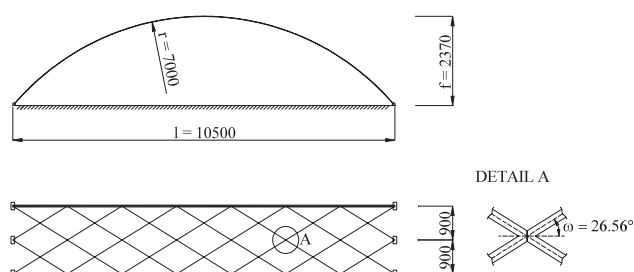


Figure 1 Basic dimensions of the modelled structure made of PVC tubes
Obrázok 1 Základné rozmery modelovanej konštrukcie z PVC rúrok

The structure constitutes an arch with the radius $r = 7\,000$ mm, with the span $l = 10\,500$ mm and with the camber $f = 2\,370$ mm. The configuration of the PVC tubes of the model is obvious from the scheme shown in Figure 1 (below). The tubes are fixed to the ground by the steel anchors. The arch consists of two sections with a width of 900 mm each, while the strength of the next possible consequent section is ensured by hardening on the ends as highlighted by bold lines.

In the paper (Páleš a Priecel, 2009), we computed the described model as the three-joint arch loaded by the self-weight. Such static scheme is featured by static certainty.

The paper (Páleš a Balková, 2011a) presents once statically uncertain system of the two-joint arch. Its calculation was more complicated as previous.

The most complex calculation was performed in the paper (Páleš a Balková, 2011b). Three times statically uncertain system of the double fixed arch forced to solve a system of three equations in three unknowns.

In this contribution, we made efforts to summarise in details all obtained theoretical results from the mathematical simulation of the structure. Later, we would like to compare these values with possible practical values measured on a laboratory model.

Materials and methods

The structure was mathematically modelled with self-weight loading. Taking into account the nature of the self-weight load, we considered the coverage of the structure made of sheets of 12104 quality according to STN (Slovak Technical Standard) 42 6882 apart from the weight of PVC tubes. The dimensions of one sheet plate are $610 \times 80 \times 1.5$ mm and its weight stated in (Hořejší a Šafka, 1987) is 21.25 kg/m^2 .

Figure 2 shows the statically certain scheme of the structure as the three-joint arch. Further statically uncertain

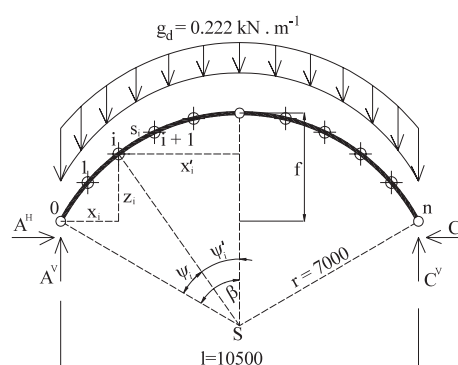


Figure 2 Computation parameters of the arch in the statically certain scheme of the three-joint arch

Obrázok 2 Výpočtové parametre oblúka na staticky určitej schéme trojklbového oblúka

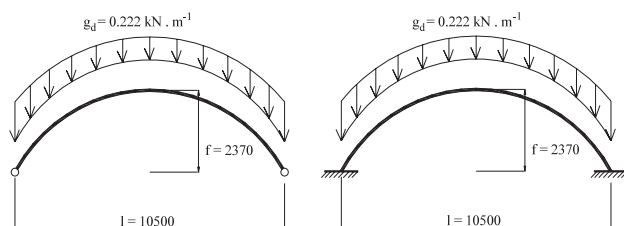


Figure 3 Statically uncertain schemes of the structure: two-joint arch and double fixed arch and their self-weight loads

Obrázok 3 Staticky neurčité schémy konštrukcie: dvojkľbový oblúk a obojstranne votknutý oblúk a ich zaťaženie vlastnou tiažou

schemes of the two-joint arch and double fixed arch are presented in Figure 3. The principle of mathematical approach to the arch geometry is the same in all three schemes.

Figure 2 shows that the computed value of self-weight load was $g_d = 0.222 \text{ kN/m}$. We computed the angle β from the selected span $l = 10\,500 \text{ mm}$ and the radius of arch $r = 7\,000 \text{ mm}$:

$$\sin \beta = \frac{l}{2 \cdot r} \quad (1)$$

The camber is calculated as follows:

$$f = r \cdot (1 - \cos \beta) \quad (2)$$

Total length of arch:

$$s = 2 \cdot r \cdot \beta \cdot \frac{\pi}{180} \quad (3)$$

We divided the whole arch into $n = 2\,000$ segments. The length of one segment was assigned as:

$$\Delta s = \frac{s}{n} \quad (4)$$

We found the angle ψ'_i as partition of the angle β to $n/2 = 1\,000$ segments:

$$\psi'_i = \beta - \frac{2 \cdot i \cdot \beta}{n} \quad (5)$$

Coordinate x'_i :

$$x'_i = \sin \psi'_i \cdot r \quad (6)$$

Coordinate z of the i segment:

$$z_i = f - r \cdot (1 - \cos \psi'_i) \quad (7)$$

Three-joint arch

In case of the three-joint arch, we computed reactions by the substitution of continuous load to alone loads over separate segments and by consecutive summation. We determined reactions A^V, A^H, C^V, C^H (Fig. 2) using the moment conditions of equilibrium toward end joints and middle joint, and using an addition condition of equilibrium. In the sense of convention for internal forces shown in Figure 4, there were specified the values of bending moment M_i , shear force T_i and normal force N_i by summation over the separate segments. We used the same convention in the next two statically uncertain systems.

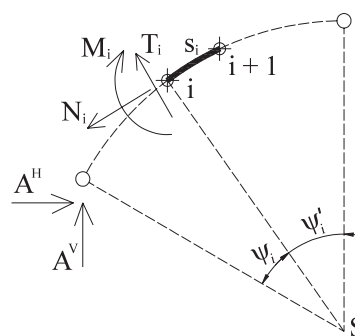


Figure 4 The convention of positive internal forces on the arch from the left

Obrázok 4 Konvencia kladných vnútorných síl na oblúku zľava

Two-joint arch

Considering the two-joint arch, we chose the first statically certain scheme according to Figure 5 (left). The horizontal reaction in right support was replaced by unit force. We calculated reactions and internal forces caused by self-weight load in the statically certain scheme. Using the same scheme we stated reactions and internal forces from the unit force X_1 . Once statically uncertain system is solved by the equation:

$$\delta_{11} \cdot X_1 + \delta_{10} = 0 \quad (8)$$

where:

δ_{11} and δ_{10} – deformation coefficients defined from moment developments in the statically certain system according to the integrals

$$\delta_{11} = \int_0^s \frac{M_1 \cdot M_1}{E \cdot J} ds \quad \delta_{10} = \int_0^s \frac{M_1 \cdot M_0}{E \cdot J} ds \quad (9)$$

M_1 is the bending moment from unit force X_1 , M_0 is the bending moment from the self-weight load, E is the modulus of elasticity, J is the moment of inertia and s is the length of the arch. The computation of (9) was performed by numerical integration because the development of moments was not in any case linear and, therefore, the known Vereshchagin rule cannot be used. By obtaining the variable X_1 from (8) we stated the internal forces by the following formulas:

$$M = M_0 + X_1 \cdot M_1 \quad (10)$$

$$T = T_0 + X_1 \cdot T_1$$

$$N = N_0 + X_1 \cdot N_1$$

Details can be found, for example, in (Novák et al., 1965).

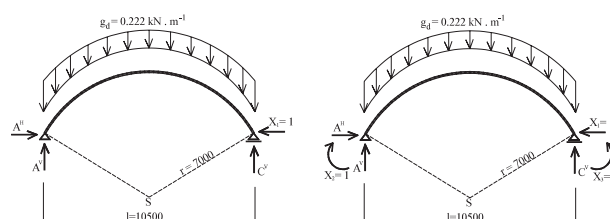


Figure 5 Basic statically certain schemes for the two-joint arch and for the double fixed arch

Obrázok 5 Základné staticky určité systémy pre dvojkľbový oblúk a pre obojstranne votknutý oblúk

Double fixed arch

The double fixed arch results in three times uncertain static system. Basic statically certain scheme was selected according to Figure 5 (right). The horizontal reaction in the right support and moments in both supports were replaced by the unit forces. We computed reactions and internal forces (bending moment, shear force and normal force) from self-weight load on the statically certain scheme. On the same scheme, we assigned reactions and internal forces from unit forces X_1 , X_2 , X_3 . For the solution of the three times uncertain system we had to form three equations in three unknowns:

$$\begin{aligned}\delta_{11} \cdot X_1 + \delta_{12} \cdot X_2 + \delta_{13} \cdot X_3 + \delta_{10} &= 0 \\ \delta_{21} \cdot X_1 + \delta_{22} \cdot X_2 + \delta_{23} \cdot X_3 + \delta_{20} &= 0 \\ \delta_{31} \cdot X_1 + \delta_{32} \cdot X_2 + \delta_{33} \cdot X_3 + \delta_{30} &= 0\end{aligned}\quad (11)$$

where:

δ_{ik} and δ_{i0} , $i = 1, 2, 3$ and $k = 1, 2, 3$ represent deformation coefficients stated from relevant moment developments in the statically certain system. Index 0 means self-weight load:

$$\delta_{ik} = \int_0^s \frac{M_i \cdot M_k}{E \cdot J} ds \quad \delta_{i0} = \int_0^s \frac{M_i \cdot M_0}{E \cdot J} ds \quad (12)$$

The meaning of the denotation is the same as the denotation used in Formula (9). There is a difference consisting of several unknowns X_1 , X_2 , X_3 and indexes i and k corresponding to them. The enumeration of integration was done numerically. We neglected the influence of shear and normal forces to the deformation of the system. By solving equation system (11) we found values X_1 , X_2 , X_3 . Resulting reactions and internal forces were obtained using the following relations:

$$\begin{aligned}A^V &= A_0^V + X_1 \cdot A_1^V + X_2 \cdot A_2^V + X_3 \cdot A_3^V \\ A^H &= A_0^H + X_1 \cdot A_1^H + X_2 \cdot A_2^H + X_3 \cdot A_3^H \\ C^V &= C_0^V + X_1 \cdot C_1^V + X_2 \cdot C_2^V + X_3 \cdot C_3^V\end{aligned}\quad (13)$$

$$\begin{aligned}M &= M_0 + X_1 \cdot M_1 + X_2 \cdot M_2 + X_3 \cdot M_3 \\ T &= T_0 + X_1 \cdot T_1 + X_2 \cdot T_2 + X_3 \cdot T_3 \\ N &= N_0 + X_1 \cdot N_1 + X_2 \cdot N_2 + X_3 \cdot N_3\end{aligned}\quad (14)$$

We would like to mention even checks performed for the correct computation of the deformation coefficients δ_{ik} and δ_{i0} , $i = 1, 2, 3$ and $k = 1, 2, 3$. The deformation coefficients result from the following relations:

$$\begin{aligned}\delta_{11} + \delta_{12} + \delta_{13} &= \delta_{1s} \\ \delta_{21} + \delta_{22} + \delta_{23} &= \delta_{2s} \\ \delta_{31} + \delta_{32} + \delta_{33} &= \delta_{3s}\end{aligned}\quad (15)$$

where:

$$\delta_{1s} = \int_0^s \frac{M_1 \cdot M_s}{E \cdot J} ds \quad \delta_{2s} = \int_0^s \frac{M_2 \cdot M_s}{E \cdot J} ds \quad \delta_{3s} = \int_0^s \frac{M_3 \cdot M_s}{E \cdot J} ds \quad (16)$$

and

$$Ms = M_1 + M_2 + M_3 \quad (17)$$

The second check consists of addition:

$$\begin{aligned}\delta_{1s} + \delta_{2s} + \delta_{3s} &= \delta_{ss} \\ \delta_{10} + \delta_{20} + \delta_{30} &= \delta_{s0}\end{aligned}\quad (18)$$

where:

$$\delta_{ss} = \int_0^s \frac{M_s^2}{E \cdot J} ds \quad \delta_{s0} = \int_0^s \frac{M_s \cdot M_0}{E \cdot J} ds \quad (19)$$

Finally, the third check results from the integration of formulas:

$$\int_0^s \frac{M_1 \cdot M}{E \cdot J} ds = 0 \quad \int_0^s \frac{M_2 \cdot M}{E \cdot J} ds = 0 \quad \int_0^s \frac{M_3 \cdot M}{E \cdot J} ds = 0 \quad (20)$$

where:

M – is a resulting development of the bending moment in the statically uncertain system. Other denotation was explained hereinbefore. Again, we refer to (Novák et al., 1965) for details

Results and discussion

Tables 1, 2, 3 present the values of internal forces, bending moment M_i , shear force T_i and normal force N_i determined in each two hundredth segment for all cases: three-joint arch, two-joint arch and double fixed arch.

Table 1 The values of internal forces calculated in each two hundredth segment on the three-joint arch

i	M_i in kN · m	T_i in kN	N_i in kN
0	0	-0.152321	-1.890742
200	-0.112719	-0.019263	-1.691614
400	-0.098733	0.033293	-1.545114
600	-0.053004	0.042028	-1.443968
800	-0.014461	0.026506	-1.384489
1 000	0	0	-1.364849
1 200	-0.014461	-0.026506	-1.384489
1 400	-0.053004	-0.042028	-1.443968
1 600	-0.098733	-0.033293	-1.545114
1 800	-0.112719	0.019263	-1.691614
2 000	0	0.152321	-1.890742

Tabuľka 1 Hodnoty vnútorných síl v každom dvestom dieliku na trojkĺbovom oblúku

Table 2 The values of internal forces calculated in each two hundredth segment in the two-joint arch

i	M_i in kN · m	T_i in kN	N_i in kN
0	0	-0.131276	-1.872182
200	-0.082992	-0.018484	-1.702131
400	-0.065816	0.039018	-1.552478
600	-0.007966	0.052070	-1.435946
800	0.045500	0.034030	-1.362079
1 000	0.066501	0	-1.336789
1 200	0.045500	-0.034030	-1.362079
1 400	-0.007966	-0.052070	-1.435946
1 600	-0.065816	-0.039018	-1.552478
1 800	-0.082992	0.018484	-1.702131
2 000	0	0.131276	-1.872182

Tabuľka 2 Hodnoty vnútorných síl v každom dvestom dieliku na dvojkĺbovom oblúku

Table 3 The values of internal forces calculated in each two hundredth segment in the double fixed arch

i	M_i in kN · m	T_i in kN	N_i in kN
0	0.105327	-0.173159	-1.909119
200	-0.023443	-0.053531	-1.745609
400	-0.043312	0.011813	-1.601248
600	-0.012709	0.033487	-1.488608
800	0.024089	0.024604	-1.417122
1 000	0.039481	0	-1.392633
1 200	0.024089	-0.024604	-1.417122
1 400	-0.012709	-0.033487	-1.488608
1 600	-0.043312	-0.011813	-1.601248
1 800	-0.023443	0.053531	-1.745609
2 000	0.105327	0.173159	-1.909119

Tabuľka 3 Hodnoty vnútorných síl v každom dvestom dieliku na obojstranne votknutom oblúku

Table 4 compares extreme bending moments and normal forces for all three static systems. Shear forces were used only to verify the calculation and were not applied to determine the normal stresses.

Table 4 Comparison of extreme bending moments and normal forces for three static systems

	Three-joint arch (1)	Two-joint arch (2)	Double fixed arch (3)
M_{\max} in kN.m	0	0.066501	0.105327
M_{\min} in kN.m	-0.115806	-0.085551	-0.045140
N_{\max} in kN	-1.364849	-1.336789	-1.392633
N_{\min} in kN	-1.890742	-1.872182	-1.909119

Tabuľka 4 Porovnanie extrémnych ohybových momentov a normálových síl pre tri statické systémy (1) trojkĺbový oblúk, (2) dvojkĺbový oblúk, (3) obojstranne votknutý oblúk

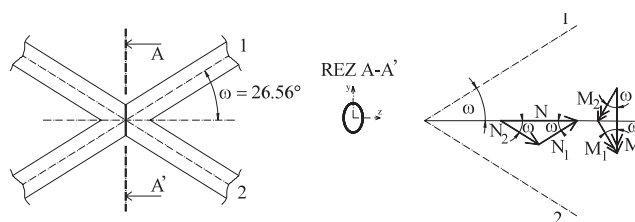
To calculate the resulting normal stresses we used the circular cross-section of PVC tube with the outside diameter of 50 mm and thickness of 2 mm. The elliptical cross-section (Prieceľ, 1982; Prieceľ a Páleš, 2008) originates in the points of tube crossing, as it can be seen from Figure 1, detail A, and from Figure 6, left. Table 5 presents the geometric parameters of the circular and elliptical cross-section as well.

Table 5 Geometric parameters, area A , moment of inertia I_y and section modulus W_y for circular and elliptical cross-sections

	A in mm ²	I_y in mm ⁴	W_y in mm ³
Circular cross-section (1)	301.59289	87 009.55	3 480
Elliptical cross-section (2)	337.1763	97 275.36	3 891.0144

Tabuľka 5 Geometrické charakteristiky, plocha A , moment zotrvačnosti I_y a prierezový modul W_y , kruhového a eliptického prierezu (1) kruhový prierez, (2) eliptický prierez

By calculating the stress in the circular cross-section we had to divide the bending moment M as well as the normal force N by the value $2 \cdot \cos \omega$, because the computed stress extends

**Figure 6** Elliptical cross-section in the cross point of two tubes and repartitioning of bending moment M and normal force N to two skewed tubes**Obrázok 6** Eliptický prierez pri krížení dvoch rúrok a prerozdelenie ohybového momentu M a normálovej sily N do dvoch zošikmených rúrok

to two skewed tubes, from which each one is deflected from the direct axis by the angle $\omega = 26.56^\circ$ (Figure 6).

Final formulas for the calculation of normal stresses in circular and ellipsoidal cross-sections are as follows:

$$\sigma_c = \frac{N}{2 \cdot \cos \omega \cdot A} \pm \frac{M}{2 \cdot \cos \omega \cdot W_y} \quad (21)$$

$$\sigma_{el} = \frac{N}{A} \pm \frac{M}{W_y} \quad (22)$$

Table 6 presents a comparison of the extreme normal stresses for three-joint arch, two-joint arch and double fixed arch for both cross-section types (circular and elliptical).

Table 6 Comparison of extreme stresses in the circular and elliptical cross-sections of the three-joint, two-joint and double fixed arches

	Three-joint arch (1)	Two-joint arch (2)	Double fixed arch (3)
$\sigma_{\max c}$ in MPa	15.548275	10.661374	13.380264
$\sigma_{\min c}$ in MPa	-21.661891	-16.829049	-20.457243
$\sigma_{\max el}$ in MPa	24.876163	17.057286	21.407336
$\sigma_{\min el}$ in MPa	-34.658810	-26.926436	-32.731497

Tabuľka 6 Porovnanie extrémnych napätí pre kruhový a eliptický prierez na trojkĺbovom, dvojkĺbovom a votknutom oblúku (1) trojkĺbový oblúk, (2) dvojkĺbový oblúk, (3) obojstranne votknutý oblúk

The scheme of the two-joint arch for self-weight load seems to be the most appropriate static scheme taking into account the minimisation of the stresses in the tubes. The stresses in Table 6 are lower for both types of cross-sections (circular and elliptical) as well as for both types of strains: negative pressure and positive tension. The double fixed arch allocated higher stresses which were a bit lower than for the three-joint arch. Considering the computation process, the double fixed arch presents the most difficult case because it results in three times statically uncertain scheme which requires considerably complicated solution. On the contrary, the three-joint arch results in the statically certain system which enables easier calculation. The two-joint arch presents once statically uncertain scheme.

Taking into account the results, it is obvious that the anchoring of all laboratory models to the ground avoids a necessity to perform hard assembling and to prevent the rotation, excluding the shift. The free anchors enabling a rotation of the arches seem to be preferable. The static

system of the three-joint arch can be considered as the worst case not only because of the highest stresses. Another issue consists of a requirement to create a joint on the top of arch.

Conclusions

We compared three different static models of arch made of polyvinylchloride tubes. By self-weight loading the model of the two-joint arch demonstrates the lowest values of stresses. The double fixed arch developed higher stresses in the tubes and their contact points. The three-joint arch appeared to be the most unfavourable case due to the highest values of stresses considering the both types of cross-sections as well as the both types of strains.

Súhrn

Obsahom článku je výpočet napätí od vlastnej tiaže strešno-stropnej oblúkovej konštrukcie z polyvinylchloridových (PVC) rúrok. Vytvorili sme koncepčný návrh takejto konštrukcie (Priecel a Páleš, 2008). Po definovaní úplnej geometrie sme vypočítali hodnotu zaťaženia vlastnou tiažou rúrok a pokrývajúcim plechom. Model sme matematicky simulovali s rôznymi okrajovými podmienkami: ako trojkĺbový oblúk (Páleš a Priecel, 2009), ako dvojklbový oblúk (Páleš a Balková, 2011 a) a ako obojstranne votknutý oblúk (Páleš a Balková, 2011 b). Pre všetky tieto typy uložení sme zostrojili samostatné algoritmy výpočtu, ktoré po vložení veľkosti vstupného zaťaženia určili výsledné napätia v PVC rúrkach a ich spojoch. Na základe dosiahnutých napätí sa snažíme určiť najvhodnejší spôsob uchytenia konštrukcie do podlahy pri laboratórnom modelovaní. Podľa získaných výsledkov najlepším modelom sa javí dvojklbový oblúk, menej priaznivým je obojstranne votknutý oblúk a najnepriaznivejšie vyšiel trojkĺbový oblúk. Tento príspevok sumarizuje doterajšie čiastkové výsledky, ktoré sme prezentovali na vedeckých konferenciách.

Kľúčové slová: konštrukcia z polyvinylchloridových rúrok, trojkĺbový oblúk, dvojklbový oblúk, obojstranne votknutý oblúk, zaťaženie vlastnou tiažou

Acknowledgement

This research performed at the Department of Structures of the Faculty of Engineering of the Slovak University of Agriculture in Nitra was supported by the Slovak Grant Agency for Science under grant VEGA No. 1/0013/09 titled "Unconventional roof-ceiling structures of specific buildings based on plastics".

References

- HOŘEJŠÍ, J. – ŠAFKA, J. et al. 1987. Statické tabulky. Praha : SNTL.
- NOVÁK, O. – JÍLEK, A. – HARVANČÍK, J. – SOBOTA, J. 1965. Stavební mechanika, část 1, Praha : SNTL.
- PÁLEŠ, D. – BALKOVÁ, M. 2011a. Porovnanie rôznych modelov strešnostropnej oblúkovej konštrukcie z PVC rúrok. In: XVIIth International Science Conference : Construmat 2011, Košická Belá, 15. – 17. 6. 2011, s. 228 – 234. ISBN 978-80-553-0685-8.
- PÁLEŠ, D. – BALKOVÁ, M. 2011b. Votknutá oblúčová konštrukcia z PVC rúrok a jej porovnanie s inými spôsobmi uloženia. In: International Science Conference : Rural buildings 2011, Nitra, 8. – 9. 9. 2011, s. 122 – 127. ISBN 978-80-552-0644-8.
- PÁLEŠ, D. – PRIECEL, J. 2009. Zataženie vlastnou tiažou strešno-stropnej lamelovej konštrukcie z PVC rúrok. In: XVth International Science Conference : Construmat 2009, Kruh u Jilemnice, 8. – 10. 6. 2009, s. 271–276. ISBN 978-80-01-04355-4.
- PRIECEL J. 1982. Použitie plastov na obalové a strešné konštrukcie poľnohospodárskych stavieb. Thesis. Nitra : SPU.
- PRIECEL, J. – PÁLEŠ, D. 2008. Strešno-stropná lamelová konštrukcia z polyvinylchloridových rúrok. In: XIVth International Science Conference : Construmat 2008, Brno, s. 93. ISBN 978-80-214-3660-2.

Contact address:

Ing. Dušan Páleš, CSc., Department of Structures, Faculty of Engineering, Slovak University of Agriculture, Tr. A. Hlinku 2, 949 76 Nitra, Slovakia, phone +421 37 641 56 95, e-mail du-san.pales@uniag.sk

Acta technologica agriculturae 4
Nitra, Slovaca Universitas Agriculturae Nitriae, 2011, s. 90–93

REDUCTION AND ELIMINATION OF ANIMAL ODOROUS SUBSTANCES REDUKOVANIE A ODSTRAŇOVANIE ŽIVOČÍŠNYCH PACHOVÝCH EMISÍ

Ivan JANOŠKO, Marián ČÉRY

Slovak University of Agriculture in Nitra, Slovakia

An effective disposal of odorous substances from dead animals greatly affects the quality of life of people in the vicinity. The removal of odorous substances is generally carried out in bio-scrubbers or thermal combustion facilities. A direct combustion of odorous gases can be carried out at temperatures around 850 °C within a few seconds. Measurements were carried out in Slovakia in accordance with the laws, rules and guidelines determining the exact procedures and methods of measurement. The level of ammonia in the combustion air is dependent on the quality of raw materials processed at rendering plants where the measurements were carried out. In order to reduce the economic costs, we would recommend the use of alternative fuels (animal fat, heavy fuel oil).

Key words: rendering plant, thermal oxidation, odour, emission

The accumulations of waste and climate changes caused by global warming of Earth's atmosphere belong to the major society's environmental problems of nowadays. This effect is called a greenhouse effect. The greenhouse effect is caused by greenhouse gases like CO₂ (carbon dioxide), NO_x (nitrogen oxide), fluorinated hydrocarbons, SF₆ (sulphur hexafluoride) and especially CH₄ (methane). The greenhouse effect occurs in a large scale and during the decomposition of organic matter deposited in municipal landfills and industrial waste, as well as during processing at rendering plants and processing wastewater.

The composition of emissions of substances can be further specified; they include a diverse mixture of organic and inorganic substances (ammonia, amines, amino acids, hydrogen sulphide / hydrogen sulphide / mercaptans, organic acids, aldehydes, ketones, etc.). In the case of odorous substances, the problem is more intractable (if unbearably malodorous substances infest population) because there are no specific emission limits defined for veterinary sanitation facilities as they are not traditional combustion plants. Therefore, in this case, there cannot be emission limits for waste incineration plants because this technology causes disposal of other input materials.

Materials and methods

The technologies for the capturing and disposal of odorous substances from processing animal waste are based on several principles, such as washing in bio-scrubbers, combustion in thermal facilities – oxidisers, or, more frequently, in equipment using ozone or active soil environment.

Operating air (Figure 1) is sucked by the fan from the collecting duct through the water absorber and bio-scrubber into the outside air. The exhaust air is forced through interlining absorbers and purifies solid particles by splashing water on the principle of counter-flow. At the first stage – bio-scrubber, the alkaline and neutral organic components of the exhaust air are neutralised and biologically removed, and ammonia is absorbed at the same time. At the second stage – bio-scrubber,

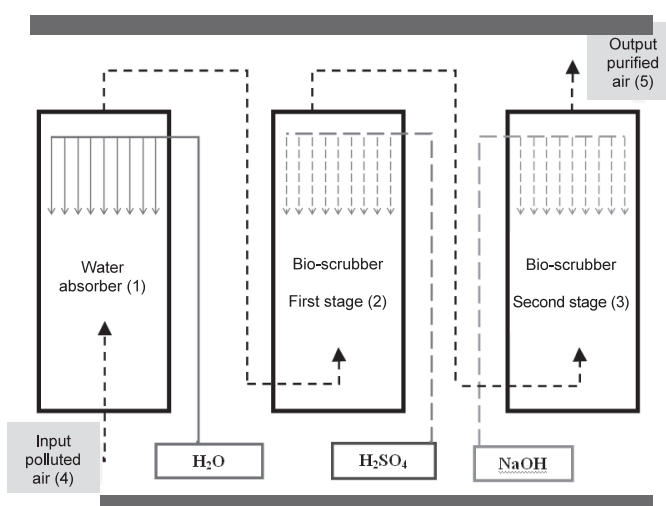


Figure 1 Multi-stage absorption column with neutralising zones
Obrázok 1 Viacstupňová absorpčná kolóna s neutralizačnými zónami
(1) vodný absorbér, (2) biopráčka – prvý stupeň, (3) biopráčka – druhý stupeň, (4) vstup znečisteného vzduchu, (5) výstup znečisteného vzduchu

acidic and neutral smelling substances are predominantly neutralised and biologically removed. The station of tanks consists of a dispenser tank of sulphuric acid, sodium hydroxide or phosphate.

Second stageSecond stageFirst stageFirst stage

A direct combustion of odorous gases (Figure 2) can be carried out at temperatures around 850 °C within a few seconds. In operation, these devices are characterised by high operating costs with regard to energy consumption. A good idea is to reduce consumption to a minimum by connecting other facilities, such as heat exchangers, etc. The system of thermal oxidation facility consists of three basic parts:

1. Combustion chamber in which gases are heated to the required temperature within the range of 850 – 1 100 °C.
2. Retention chamber in which a delay of 1 – 2 seconds is ensured for the gas oxidation process.

3. Steam boiler in which the oxidation of gases used to produce the steam can also be used in the manufacturing process technology.

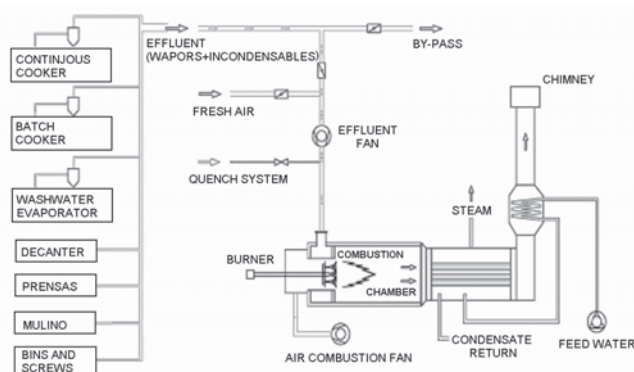


Figure 2 Flow chart of thermal oxidation facility
Obrázok 2 Bloková schéma tepelného oxidačného zariadenia

Another heat exchanger is used to preheat the combustion air and input steam into the combustion chamber. This system eliminates malodorous gases originating in the manufacturing process and in used rendering plant technology. It processes wastewater and releases it as a pure water vapour. Some sources indicate that it is not necessary to use condensing systems and sewage plants.

According to these tools, we can recommend the reduction of emissions of odorous substances:

- in small volumes with high intensity,
- in large volumes of low intensity, at almost 100% efficiency,
- exclusion of any liquids.

Measurement methods and regulations

Measurements were carried out in Slovakia in accordance with the laws, rules and guidelines determining the exact procedures and methods of measurement. The Act and Decrees of the Ministry of Environment of the Slovak Republic:

- Act No 478/2002; Decree No 706/2002, as amended,
- Decree No 408/2003; Decree No 202/2003.

Standards and methods

- ISO 9096 – Air quality. Stationary source emissions. Manual determination of mass concentration of particulate matter (PM, mass flow)
- STN EN 13526 – Air quality. Stationary source emissions. Determination of the mass concentration of total gaseous organic carbon in flue gases from solvent using processes. Continuous flame ionisation detector method
- ČSN 834728 – Air quality. Emission measurement of ammonia from stationary sources of air pollution. General part. Approved 8.10.1984, effective from 1.4.1986
- ISO 10396 – Stationary source emissions. Sampling for the automated determination of gas emission concentrations for permanently-installed monitoring systems
- STN EN 15058 – Air quality. Stationary source emissions. Determination of mass concentration of carbon monoxide (CO). Reference method: Non-dispersive infrared spectrometry
- ISO 10849 – Ambient air. Stationary source emissions. Determination of the mass concentration of nitrogen oxides.

Performance characteristics of automated measuring systems

- ISO 7935 – Stationary source emissions. Determination of the mass concentration of sulphur dioxide. Performance characteristics of automated measuring methods
- STN EN 14789 – Stationary source emissions. Determination of volume concentration of oxygen (O₂). Reference method. Paramagnetism
- STN EN 14790 – Stationary source emissions. Determination of the water vapour in ducts
- STN EN 10780 – Stationary source emissions. Measurement of velocity and volume flow rate of gas streams in ducts

Description of measurements

Analysis of waste gas components: the determination of the mass concentration of total gaseous organic carbon (TOC) was performed using an extractive sampling system for measuring emission lines – BA 3006-1. The measurement of concentrations of gaseous emissions (CO, NO_x, SO₂, O₂, CO₂) was carried out using an extractive emission sampling system – ENDA 680 P-2. The principles of measuring NO_x, SO₂, CO₂, CO using cross-flow modulated non-dispersive infrared detection and of measuring O₂ by magnetopneumatic detection are shown in Figure 3.

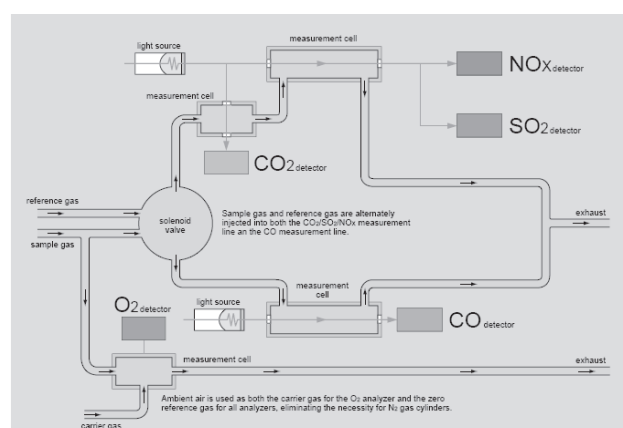


Figure 3 Flow chart of the principles of measuring gases NO_x, SO₂, CO₂, CO and O₂ using the ENDA 680 analyser (Horiba company)
Obrázok 3 Bloková schéma princípov merania plynov NO_x, SO₂, CO₂, CO and O₂ analyzátorom Enda 680 od firmy HORIBA

The determination of emissions of inorganic gaseous pollutants was performed using a suitable sampling device that corresponds to the legislative requirements of technical standards. It ensures the required flow of exhaust gas mixture through sorption columns when determining the defined volume of a sample under specified conditions.

The measurements of inorganic pollutants (NH₃) were done using a TESTO 339 pre-treatment unit. Gas was subjected to two-stage absorption in glass containers filled with a liquid sorbent – concentrated sulphuric acid solution. A sample of waste gas was taken by a pump through the control valve and float flow meter. The suction volume of the waste gas sample was measured using a laboratory meter for measuring the temperature and pressure of the sample.

Sampling for the determination of particulate matter was performed manually using a gravimetric sampling device – KS 404. The using of fuel combustion to generate the required



Figure 4 Sampling – bio-scrubber
Obrázok 4 Odber vzoriek – biopráčka

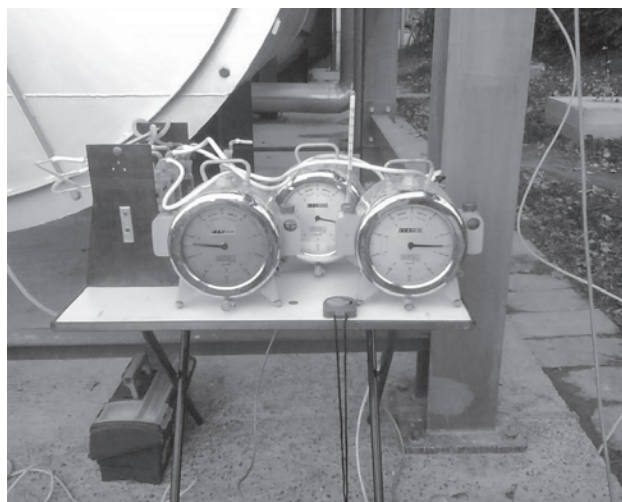
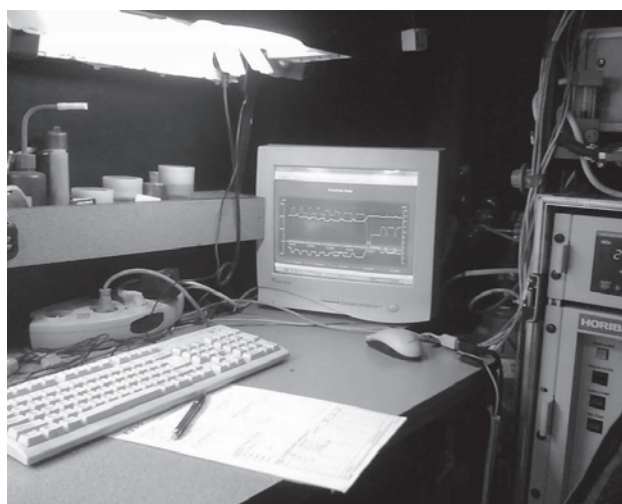


Figure 6-7 Measurement and recorded data of output gases in a computer



Obrázok 6-7 Meranie a nameraný priebeh dát výstupných plynov v počítači

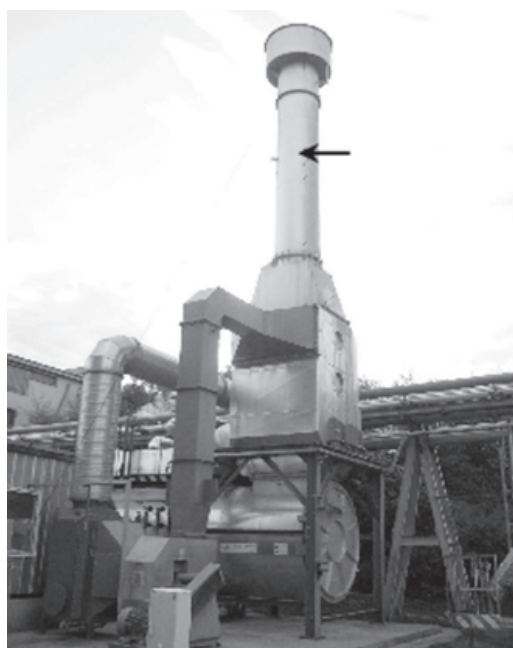


Figure 5 Sampling – oxidiser
Obrázok 5 Odber vzoriek – oxidizér

temperature is different according to the operators of combustion facilities, i.e. depending upon law in a relevant country and economic opportunities. The device enables burning different types of fuel, heavy fuel oil and animal fat; in most cases, it is mainly natural gas. The ideal situation is when we can produce fuel at our own expense, such as the rendering plant that processes the carcasses of dead animals, produces significant quantities of malodorous substances, and the resulting product is a meat, bone meal and animal fat that can be used as a fuel. The fuel obtained in this way should be cleaned from coarse impurities and delivered under pressure ensuring a perfect diffusion to aerosols (either by compressed air or steam from own production).

Results and conclusions

The values shown in Table 1 are collected from several countries during several years. We cannot exactly determine the methods, measurements and collected data in other countries, except for Slovakia in years 2006 and 2007. In these

years, measurements were performed on newly installed equipment according to standards, regulations and legislation in force in Slovakia at that time. The results were recorded at different intervals and different temperatures using different types of fuels. We also should not forget the extent of pollution of burnt air. It has a major impact on the measurement results. It is possible to evaluate the measurement results as incomprehensive and informative only. As a large number of unknown values enters the measurements, we do not have enough information needed for an accurate assessment. It is clear that the most ideal fuel is natural gas producing the least amount of ash.

The achieved level of emissions from equipment is influenced by the basic conditions of combustion and, as mentioned above, they are influenced by the fuel used and the composition and concentration of combustion gases. The concentrations of substances, such as NO_x , result from the decomposition of substances present in the combustion air. The main factor that affects the amount of NO_x emitted is the concentration of ammonia in the gas technology. The level of ammonia in the combustion air is dependent on the quality of a raw material processed at rendering plants where the measurements were carried out. That means that a fresher material means a lower production of harmful gases.

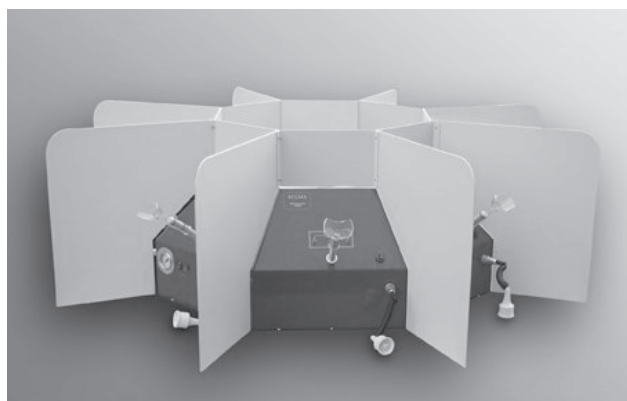
Table 1 Measured emission limits

Year (1)	Fuel (2)	T in °C (3)	O ₂ in % (4)	Concentration of gases in the reference volume of O ₂ 11 % in mg/m ³ (5)						
				C.O.T.	CO	NO ₂	SO ₂	NH ₃	HC ₁	Dust
Slovakia 2006	Gas	900	11	29	18	663	145	37	5	5
Slovakia 2007	Gas	900	11	17	2	302	109	29	–	83

Tabuľka 1 Namerané emisné limity

(1) rok, (2) palivo, (3) teplota, (4) obsah kyslíka, (5) koncentrácia plynov v referenčnom objeme kyslíka

The determination of the content and concentration of odorous substances emitted to the air was assessed through the evaluation of data obtained by a special device – olfactometer by ECOMA (Figure 8).

**Figure 8** Olfactometer T08-8 (ECOMA)**Obrázok 8** Olfaktometer T08-8 (ECOMA)

The degrees of dilution of the olfactometer were verified by the olfactometer manufacturer using the propane calibration gas diluted with synthetic air in accordance with the applicable standard ČSN EN 13725. The assessment committee is selected on the basis of a selection procedure, in which individual members passed competitions regarding the substance tested – n-butanol reference gas. Conditions in the laboratory at the time of measurement: temperature 22.4 °C, humidity 51.2 %.

Tables 2 and 3 present the results of measuring the concentration of odorous substances in accordance with Air Protection Act No 86/2002 of the Czech Republic and Decree of the Ministry of Environment No 362/2006. The final concentration of odorous substances is calculated as an average of individual samples.

The measured values of concentrations of odorous substances indicate a significant difference in the efficiency of purification of individual devices. The resulting values of odorous substances leaking from the bio-scrubber are about two orders of magnitude higher than the values of the thermal oxidiser.

Table 2 Concentration of odorous substances in samples – oxidiser

Sample (1)	Concentration of odorous substances OUE/m ³ (2)	Average concentration of odorous substances OUE/m ³ (3)
1	825	428.5
2	441	
3	362	
4	256	

Tabuľka 2 Koncentrácia pachových látok vo vzorkách – oxidizér

(1) vzorka, (2) koncentrácia pachových látok, (3) priemerná koncentrácia pachových látok

Table 3 Concentration of odorous substances in samples – bio-scrubber

Sample (1)	Concentration of odorous substances OUE/m ³ (2)	Average concentration of odorous substances OUE/m ³ (3)
1	15 024	19 184.5
2	28 774	
3	19 972	
4	15 689	

Tabuľka 3 Koncentrácia pachových látok vo vzorkách – biopráčka

(1) vzorka, (2) koncentrácia pachových látok, (3) priemerná koncentrácia pachových látok

Súhrn

Účinné zneškodňovanie pachových látok z uhynutých zvierat výrazne ovplyvňuje kvalitu života ľudí v blízkom okolí. Odstraňovanie zápachajúcich látok možno realizovať spravidla v biopráčkach alebo termálnych spaľovacích zariadeniach, prípadne ozonizéroch. Priame spaľovanie pachových plynov v zariadení pre zneškodňovanie živočíšnych odpadov možno vykonávať pri teplotách okolo 850 °C počas niekoľkých sekúnd. Meranie zneškodňovania zápachajúcich látok bolo vykonané na Slovensku v súlade so zákonmi, pravidlami a usmerneniami pre stanovenie presných postupov a metód merania. Úroveň čpavku v spaľovacom vzduchu je závislá od kvality surovín spracovaných v kafilérii, kde sa meranie vykonáva. S cieľom znížiť ekonomické náklady, odporúčame používanie alternatívnych palív (živočíšny tuk, ťažký vykurovací olej).

Kľúčové slová: kafilérie, tepelná oxidácia, zápach, emisie

Acknowledgement

This paper was prepared within the project of the Ministry of Education of the Slovak Republic VEGA No 1/0857/12 "Reduction of unfavourable impacts of agricultural and transport machinery on environment."

References

- BABCOCK WANSON GROUPE. Company materials
 ČERNECKÝ, J. – NEUPAUEROVÁ, A. – JANOŠKO, I. – SOLDÁN, M. 2010. Technika životného prostredia. Zvolen : TU, 2010. s. 272. ISBN 978-80-228-2161-2.
 ČÉRY, M. – JANOŠKO, I. 2009. Zneškodňovanie nebezpečných odpadov živočíšného pôvodu II. In: Technika odpadového hospodárstva : medzinárodný seminár, 17. september 2009, Zvolen, Slovenská republika. – Zvolen : Technická univerzita Zvolen, 2009. s. 30 – 36. ISBN 978-80-228-2027-1.
 ČÉRY, M. – JANOŠKO, I. 2010. Emission Produced by the Combustion of Odour Substances in Thermo-oxidative Device. In: Nové trendy v technike ochrany ovzdušia : medzinárodný seminár, 16. jún 2010, Zvolen, Slovenská republika. – Zvolen : Technická univerzita Zvolen, 2010. s. 24 – 31. ISBN 978-80-228-2117-9.

ČSN EN 13725. Air quality – Determination of odour concentration by dynamic olfactometry

ČSN ISO 10780. Stationary source emissions. Measurement of velocity and volume flow rate of gas streams in ducts

HOSTÍN, S. 2010. Využitie ozonizácie pre redukciu emisii prchavých látok do ovzdušia. In: Nové trendy v technike ochrany ovzdušia : medzinárodný seminár, 16. jún 2010, Zvolen, SR. Zvolen : Technická univerzita, 2010. s. 41 – 47. ISBN 978-80-228-2117-9.

KNÍŽATOVÁ, M. – MIHINA, Š. – KARANDUŠOVSKÁ, I. – ORSÁG, J. – ŠOTTNÍK, J. 2009. Koncentrácie a emisie amoniaku a skleníkových plynov v chove brojlerových kurčiat v letnom období a ich závislosť od vybraných vlastností podstielky. In: Acta technologica agriculturae, roč. 12, č. 1, s. 1 – 5. ISSN 1335-2555.

KNÍŽATOVÁ, M. – MIHINA, Š. – ORSÁG, J. – KARANDUŠOVSKÁ, I. 2010. Vplyv stavu podstielky a intenzity vetrania na emisie amoniaku a oxidu uhličitého pri výkrme kurčiat. In: Acta technologica agriculturae, roč. 13, č. 1, s. 22 – 27. ISSN 1335-2555.

ÖSKO. Company materials

PECIAR, M. – ČERNECKÝ, J. – PECIAROVÁ, Z. 2011. Ochrana ovzdušia – meranie a monitorovanie. Bratislava : Nakladateľstvo STU, 2011. s. 136. ISBN 978-80-227-3392-2.

TOP-ENVI-Tech Brno.: Company materials

Contact address:

doc. Ing. Ivan Janoško, CSc., Department of Transport and Handling, Faculty of Engineering, Slovak University of Agriculture in Nitra, Štefániková trieda 56, 949 01 Nitra, e-mail: Ivan.Janosko@uniag.sk

Acta technologica agriculturae 4
Nitra, Slovaca Universitas Agriculturae Nitriae, 2011, s. 94–97

MECHANICAL PROPERTIES OF VISCOELASTIC FOILS MECHANICKÉ VLASTNOSTI VISKOELASTICKÝCH FÓLIÍ

Lubomír KUBÍK, Stanislav ZEMAN

Slovak University of Agriculture in Nitra, Slovakia

The paper deals with the mechanical properties, such as the tensile diagram, stress, strain, modulus of elasticity and stress and strain at the rupture, of thin (thickness of 50 µm) foils containing 91 % of polyethylene Bralen RA 2-63 and 9 % coloured concentrate of Maxithen and polypropylene nonwoven fabric black foil Biotex PP – UV 71031. The foils are used in mulch applications in agriculture. Four sorts of foils were examined: samples with Maxithen HP 1510 – white, Maxithen HP 231111 – yellow, Maxithen HP 533031 – blue and polypropylene nonwoven fabric black foil Biotex PP – UV 71031. Longitudinal and transversal tensile properties were studied. The tensile behaviour was monitored on the motorised test stand ANDILOG STENTOR 1000. The moduli of elasticity of longitudinal samples of polyethylene Bralen RA 2-63 foils achieved the values in the range from 222.73 MPa to 250.92 MPa and transversal samples in the range from 179.61 MPa to 270.41 MPa. The moduli of elasticity of polypropylene nonwoven fabric black foil Biotex PP – UV 71031 of longitudinal samples were 64.76 MPa and transversal samples 91.66 MPa. The stress of longitudinal samples of polyethylene Bralen RA 2-63 foils at the rupture achieved the values in the range from 9.46 MPa to 13.33 MPa at the strain from 1.51 mm/mm to 1.54 mm/mm and transversal samples in the range from 12.16 MPa to 15.54 MPa at the strain from 1.51 mm/mm to 1.58 mm/mm. The stress of longitudinal samples of polypropylene nonwoven fabric black foil Biotex PP – UV 71031 at the rupture was 4.73 MPa at strain 1.36 mm/mm and transversal samples 7.17 MPa at strain 1.52 mm/mm.

Key words: tensile modulus of elasticity, viscoelasticity, polyethylene foil, polypropylene foil

Thin plastic films are used in a wide variety of applications such as packaging materials, heat shrink wrap, consumer plastic bags, and adhesive tape. The end use of a thin plastic film may require either high stretching (food wrap) or low stretching (protective coatings). Tensile modulus is the measure of a film resistance to stretching and therefore is an important property to correlate with end-use performance (Foreman et al., 1997).

Polyethylene plastic foils used in horticulture are of great importance. Plastic foils used as mulch affect the radiation balance of the environment by means of absorption and reflection of light by their surface, and they change the microclimate of cultivated plants. The colour of foils influences the temperature of foils and layer of the soil lying below it. Mulch modifies microclimate by increasing the soil temperature and reflectivity while decreasing the soil water and nutrient losses. Black foils absorb most ultraviolet, visible and infrared

wavelengths of incoming radiation. Compared to bare soil, daytime temperature is higher at the 5 cm depth by approximately 5 °C and by 3 °C at the 10 cm depth. White foils reflect radiation with the soil temperature resulting in a slight decrease of -0.7 °C at the 10 cm depth. Blue has been shown to increase the muskmelon, cucumber and summer squash yield by 20 to 30 per cents over 3 years in trials at the Penn State Center for Plasticulture (Taber, 2010). Foils evoke more favourable conditions of the growing and progression of plants, the consequence of which is the enhancing of harvest, quality and realised production (Romic et al., 2003; Ibarra-Jimenez et al., 2006). Fruiting vegetables have a best response to the application of foils. The mechanical properties of plastic foils are important for the determination of suitable mulch foils for various plants as regards the penetration of plants through mulch foils. The objective of this study was to examine the

tensile behaviour of various thin foil plastic materials and to measure the modulus in the linear region.

Materials and methods

Samples containing 91 % of Bralen RA 2-63 polyethylene and 9 % coloured concentrate of Maxithen. They were made by Plastika a.s. Nitra for mulch applications. Four sorts of foils were examined: samples with Maxithen HP 1510 – white, Maxithen HP 231111 – yellow, Maxithen HP 533031 – blue and polypropylene nonwoven fabric black foil Biotex PP – UV 71031. The thickness of samples was 50 μm . Examinations were performed according to Standard STN ISO 527 – 1, 2, 3. Samples were cut in the longitudinal and transversal direction on the dimensions of (150 \times 15) mm. Ten samples of foils were used of each sort. In this test, load was applied along the longitudinal axis of a circular test specimen. The applied load and the resulting elongation of the member were measured. The process was repeated with increased load until the desired load levels were reached or the specimen breaks. The tensile behaviour was monitored on the motorised test stand ANDILOG STENTOR 1000 with maximal reached force about 9 – 12 N (Figure 1). The force F (N) and elongation Δl (mm) were measured when the speed of flat grip fixtures was 200 $\text{mm}\cdot\text{min}^{-1}$, and data were stored in the xls format in the computer. The force and elongation were transformed by means of software Microsoft Office Excel 2003 to the tensile stress σ (MPa) and strain ε (mm/mm). Tensile stresses σ (MPa) were determined from equation (1):

$$\sigma = \frac{F}{S} \quad (1)$$

where F (N) is force and S (mm^2) is an initial cross section of foils. Strains ε (mm/mm) were determined as a change in the specimen gage length from equation (2):

$$\varepsilon = \frac{\Delta l}{L_0} \quad (2)$$

where Δl (mm) is the gain distance between grips and L_0 is an initial length of the sample 150 mm. The tensile modulus of elasticity E (MPa) is defined as the

stress change divided by the change in strain within the linear region of stress-strain curves (3):

$$E = \frac{\sigma_2 - \sigma_1}{\varepsilon_2 - \varepsilon_1} \quad (3)$$

where σ_1 is the stress equivalent the strain $\varepsilon_1 = 0.0005$, and σ_2 is the stress equivalent the strain $\varepsilon_2 = 0.0025$. Modulus values were calculated by taking the slope of stress versus strain curves but only in the range of strains from 0.0005 to 0.0025 (0.05 – 0.25 %) where the stress-strain relationship is linear (STN ISO 527-1). The breaking strength determined by σ_b (MPa) and ε_b (mm/mm) were also measured in the time of the rupture of foils

Results and discussion

At low stresses, the most samples indicated a linear viscoelastic response. The example of a tensile stress-strain diagram of the longitudinal polyethylene foil sample with coloured concentrate Maxithen HP 231111 – white are presented in Figure 2. The relationship presents the region of linear viscoelasticity to the value of strain 0.0025 mm/mm, then the region of viscoelasticity to the value of strain about 0.060 mm/mm and the region of plasticity over strain 0.060 mm/mm.

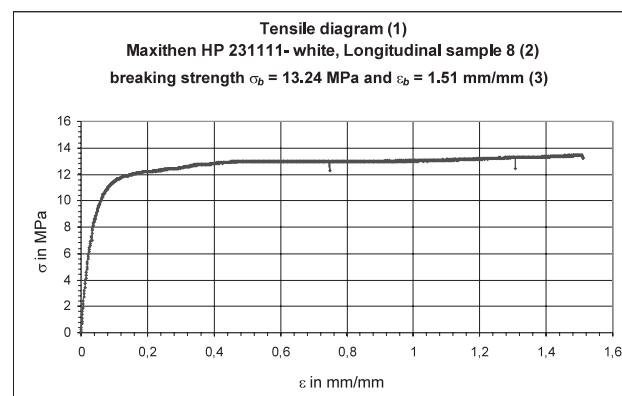


Figure 2 Tensile stress – σ /strain – ε diagram of polyethylene sample Bralen RA 2-63 with Maxithen HP 23111 colour concentrate – white for longitudinal sample 8 and the values of breaking strength $\sigma_b = 13.24$ MPa and $\varepsilon_b = 1.51$ mm/mm

Obrázok 2 Ťahový diagram napätie – σ /deformácia – ε polyetylénovej vzorky Bralen RA 2-63 s farebným koncentrátom Maxithen HP 23111 – biela pre pozdĺžnu vzorku 8 a hodnoty napätia a deformácie pri pretrhnutí $\sigma_b = 13,24$ MPa a $\varepsilon_b = 1,51$ mm/mm (1) ťahový diagram, (2) Maxithen HP 23111 – biela, pozdĺžna vzorka 8, (3) napätie $\sigma_b = 13,24$ MPa a deformácia $\varepsilon_b = 1,51$ mm/mm pri pretrhnutí



Figure 1 Test stand Andilog Stentor 1000 with the foil sample
Obrázok 1 Testovacie zariadenie Andilog Stentor 1000 so vzorkou fólie

The breaking strength is determined by stress 13.24 MPa and strain 1.51 mm/mm. The resulting modulus of elasticity observed in Figure 3 was 296.65 MPa. The tensile diagram of polypropylene nonwoven fabric black foil Biotex PP – UV 71031 for transversal sample 6 and the values of breaking strength $\sigma_b = 7.26$ MPa and $\varepsilon_b = 1.51$ mm/mm are presented in Figure 4. The modulus of elasticity $E = 102.25$ MPa of polypropylene nonwoven fabric black foil Biotex PP – UV 71031 for transversal sample 6 was detected from the relationship shown in Figure 5.

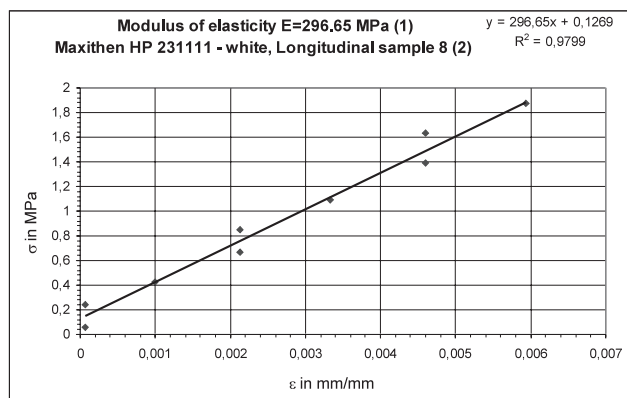


Figure 3 Determination of modulus of elasticity $E = 296.65$ MPa in the linear strain region of polyethylene longitudinal sample 8 Bralen RA 2-63 with Maxithen HP23111 colour concentrate – white

Obrázok 3 Stanovenie modulu pružnosti $E = 296.65$ MPa v lineárnej oblasti deformácie polyetylénovej pozdĺžnej vzorky 8 Bralen RA 2-63 s farebným koncentrátom Maxithen HP 23111 – biela (1) modul pružnosti $E = 296.65$ MPa, (2) Maxithen HP 23111 – biela, pozdĺžna vzorka 8

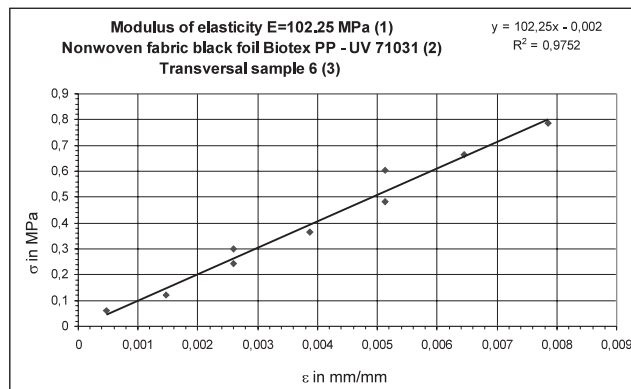


Figure 5 Determination of modulus of elasticity $E = 102.25$ MPa in the linear strain region of polypropylene nonwoven fabric black foil Biotex PP – UV 71031 for transversal sample 6

Obrázok 5 Stanovenie modulu pružnosti $E = 102.25$ MPa v lineárnej oblasti deformácie čiernej polypropylénovej netkanej textílie Biotex PP – 71031 pre priečnu vzorku 6 (1) modul pružnosti $E = 102.25$ MPa, (2) čierna polypropylénová netkaná textília Biotex PP – 71031, (3) priečna vzorka 6

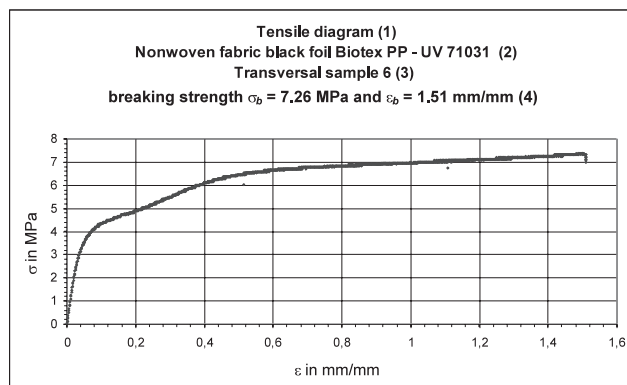


Figure 4 Tensile stress – σ /strain – ϵ diagram of polypropylene nonwoven fabric black foil Biotex PP – UV 71031 for transversal sample 6 and the values of breaking strength $\sigma_b = 7.26$ MPa and $\epsilon_b = 1.51$ mm/mm

Obrázok 4 Ťahový diagram napätie – σ /deformácia – ϵ čiernej polypropylénovej netkanej textílie Biotex PP – 71031 pre priečnu vzorku 6 a hodnoty napätia a deformácie pri pretrhnutí $\sigma_b = 7.26$ MPa a $\epsilon_b = 1.51$ mm/mm (1) Ťahový diagram, (2) čierna polypropylénová netkaná textília Biotex PP – 71031, (3) pozdĺžna vzorka 6, (4) napätie $\sigma_b = 7.26$ MPa a deformácia $\epsilon_b = 1.51$ mm/mm pri pretrhnutí

The results of the examined foils for the longitudinal and transversal samples are presented in Table 1 and Table 2, respectively.

The mean values of the moduli of elasticity of longitudinal and transversal samples exhibited similar size. There were not significant differences among the values of the longitudinal and transversal properties of plastic foils. The mean values of polyethylene Bralen RA 2-63 were different in comparison with the mean values of polypropylene nonwoven fabric black foil Biotex PP – UV 71031 in the moduli of elasticity, and values characterised rupture σ_b and ϵ_b . The measurements of polypropylene nonwoven fabric black foil Biotex PP – UV 71031 resulted in the lowest mean values characterising the rupture properties of foils σ_b and ϵ_b . The highest standard deviation was obtained from the measurement of the modulus of elasticity of longitudinal samples of polypropylene nonwoven fabric black foil Biotex PP – UV 71031. However, the values were determined from ten samples of the foil. A smaller precision was probably induced by the problems with the measurement and recording of the initial values of force and elongation by the test stand Andilog. Polypropylene nonwoven fabric black foil Biotex PP – UV 71031 was less elastic and less strong than Bralen RA 2-63. The moduli of the polyethylene material occurred within the expected range of 55 MPa to 172 MPa (Brandrup et al., 1999).

Table 1 Results of the modulus of elasticity E (MPa), the stress and strain in the moment of rupture σ_b (MPa) and ϵ_b (mm/mm) of longitudinal samples and their standard deviations for the yellow, white and blue plastic foils Bralen RA 2-63 and polypropylene nonwoven fabric black foil Biotex PP – UV 71031

Sample (1)	Longitudinal (2)					
	mean (3) E (MPa)	Std (4) s_E (%)	mean (3) σ_b (MPa)	Std (4) s_{σ} (%)	mean (3) ϵ_b (mm/mm)	Std (4) s_{ϵ} (%)
Yellow (5)	250.92	5.4	12.55	0.95	1.54	1.64
White (6)	222.73	8.04	13.33	0.91	1.51	0.49
Black (7)	64.76	19.95	4.73	5.55	1.36	2.10
Blue (8)	228.87	12.10	9.46	1.09	1.51	0.84

Tabuľka 1 Výsledky modulu pružnosti v ťahu E (MPa), napätia a deformácie v momente pretrhnutia vzorky σ_b (MPa) a ϵ_b (mm/mm) pozdĺžnych vzoriek a ich štandardné odchýlky pre žltú, bielu a modrú polyetylénovú fóliu Bralen RA 2-63 a čiernu polypropylénovú netkanú textíliu Biotex PP-71031 (1) vzorka, (2) pozdĺžna, (3) priemer, (4) štandardná odchýlka, (5) žltá, (6) biela, (7) čierna, (8) modrá

Table 2 Results of the modulus of elasticity E (MPa), the stress and strain in the moment of rupture σ_b (MPa) and ε_b (mm/mm) of transversal samples and their standard deviations for the yellow, white and blue plastic foils Bralen RA 2-63 and polypropylene nonwoven fabric black foil Biotex PP – UV 71031

Sample (1)	Transversal (2)					
	mean (3) E (MPa)	Std (4) s_E (%)	mean (3) σ_b (MPa)	Std (4) s_σ (%)	mean (3) ε_b (mm/mm)	Std (4) s_ε (%)
Yellow (5)	270.41	7.50	12.16	0.89	1.58	0.60
White (6)	179.61	13.31	15.54	0.70	1.51	0.24
Black (7)	91.66	7.62	7.17	0.96	1.52	0.29
Blue (8)	207.89	10.26	13.00	0.68	1.51	0.67

Tabuľka 2 Výsledky modulu pružnosti v ťahu E (MPa), napätia a pozdĺžneho pomerného predĺženia v momente pretrhnutia vzorky σ_b (MPa) a ε_b (mm/mm) priečných vzoriek a ich štandardné odchýlky žltej, bielej a modrej plastickej fólie Bralen RA 2-63 a čiernej polypropylénovej netkanej textílie Biotex PP – 71031

(1) vzorka, (2) priečna, (3) priemer, (4) štandardná odchýlka, (5) žltá, (6) biela, (7) čierna, (8) modrá

Conclusions

The tensile properties of polyethylene and polypropylene foils are important for the assessment of a mechanical condition of materials. The tensile properties of foils were studied only in the linear viscoelastic region of foil deformations. The viscoelastic behaviour of polymers depends not only on the temperature but also on the time. The stress-strain relationship of the tensile test is nonlinear even in the range of linear viscoelasticity. This effect is typical for tenacious polymers. For that reason, the values of the tangential modulus of tenacious materials, determined from the initial part of the stress-strain curve, often depend on the applied scale factor. Therefore, the method of measuring the modulus of elasticity was based on two specific values of strain, i.e. 0.05 % and 0.25 %.

Súhrn

Práca sa zaoberá štúdiom mechanických vlastností – ťahový diagram, napätie, deformácia, modul pružnosti a napätie a deformácia v okamihu pretrhnutia – tenkých (hrúbka 50 μm) polyetylénových fólií zložených z 91 % polyetylénu Bralen RA 2-63 a 9 % farebného koncentrátu Maxithen a štúdiom čiernych polypropylénových netkaných textílií Biotex PP – UV 71031. Fólie sú využívané na mulčovanie v poľnohospodárstve. Boli študované štyri druhy fólií: vzorky s Maxithenom HP 1510 – biele, Maxithenom HP 231111 – žlté, Maxithenom HP 533031 – modré a čierne polypropylénové netkané textílie Biotex PP – UV 71031. Ťahové vlastnosti boli zisťované pre pozdĺžne a priečne vystrihnuté vzorky. Správanie sa vzoriek pri ťahovom namáhaní bolo monitorované testovacím zariadením ANDILOG STENTOR 1000. Pri pozdĺžne polyetylénových vzorkách fólie Bralen RA 2-63 boli zistené moduly pružnosti v rozsahu od 222,73 MPa do 250,92 MPa a pri priečných vzorkách v rozsahu od 222,73 MPa do 250,92 MPa. Pre čiernu polypropylénovú netkanú textíliu Biotex PP – UV 71031 boli pre pozdĺžne vzorky zistené moduly pružnosti v ťahu 64,76 MPa a priečne vzorky 91,66 MPa. Hodnoty mechanického napätia pre pozdĺžne vzorky polyetylénu Bralen RA 2-63 v okamihu pretrhnutia vzorky boli v rozsahu od 9,46 MPa do 13,33 MPa pri zodpovedajúcich deformáciách v rozsahu od 1,51 mm/mm do 1,54 mm/mm a pre priečne vzorky v rozsahu od 12,16 MPa do 15,54 MPa pri zodpovedajúcich deformáciách od 1,51 mm/mm do 1,58 mm/mm. Napätia pozdĺžnych vzoriek čiernej polypropylénovej netkanej textílie Biotex PP – UV 71031 v okamihu pretrhnutia dosahovali hodnoty 4,73 MPa pri deformácii 1,36 mm/mm a pozdĺžne vzorky 7,17 MPa pri deformácii 1,52 mm/mm.

Kľúčové slová: modul pružnosti v ťahu, viskoelasticita, polyetylénová fólia, polypropylénová fólia

Acknowledgement

This work was supported by the Scientific Grant Agency of the Ministry of Education of the Slovak Republic and the Slovak Academy of Sciences. The paper was prepared within research project VEGA No 1/0708/09 "Research into the use of thermal energy from renewable resources in agricultural drying with respect to its impact on ecology and technology"

References

- BRANDRUP, J. – IMMERGUT, E. H. – GRULKE, E. A. eds. 1999. Polymer Handbook. 4th Ed, Wiley, New York, 1975, 2000 pp.
- FOREMAN, J. – GILL, P. S. – SAUERBRUNN, S. R. 2010. Tensile modulus of plastic films. [online] Publikované 12. 5. 1997 [Citované 22. 8. 2011]. Dostupné z http://www.tainstruments.com/main.aspx?n=2&id=181&main_id=355&siteid=11
- IBARRA-JIMENEZ, L. et al. 2006. Watermelon response to plastic mulch and row covers. In: European Journal of horticultural science, vol. 71, 2006, no 6, p. 262 – 266.
- ROMIC, D. et al. 2003. Polyethylene mulches and drip irrigation increase growth and yield in watermelon (*Citrullus lanatus* L.). In: European journal of horticultural science, vol. 68, 2003, no 4, p. 192 – 198.
- TABER, H. G. 2010. Mulches and Drip Irrigation for High Tunnels. Iowa High Tunnel Fruit and Vegetable Production Manual. [online] Publikované 18. 6. 2010. [Citované 22. 8. 2011]. Dostupné z <http://www.extension.iastate.edu/Publications/PM2098.pdf>
- STN EN ISO 527-1:1997. Plasty. Stanovenie ťahových vlastností. 1. časť. Skúšobné podmienky pre fólie a dosky. Úrad pre normalizáciu, metrológiu a skúšobníctvo SR.
- STN EN ISO 527-2:1997. Plasty. Stanovenie ťahových vlastností. 2. časť. Skúšobné podmienky pre fólie a dosky. Úrad pre normalizáciu, metrológiu a skúšobníctvo SR.
- STN EN ISO 527-3:1997. Plasty. Stanovenie ťahových vlastností. 3. časť. Skúšobné podmienky pre fólie a dosky. Úrad pre normalizáciu, metrológiu a skúšobníctvo SR.

Contact address:

RNDr. Lubomír Kubík, PhD., Department of Physics, Faculty of Engineering, Slovak University of Agriculture in Nitra, Tr. A. Hlinku 2, 949 76 Nitra, Slovak Republic, tel.: +421 37 6414879, fax: +421 37 7417 003, e-mail: Lubomir.Kubik@uniag.sk; doc. Ing. Stanislav Zeman, CSc., Department of Production Engineering, Faculty of Engineering, Slovak University of Agriculture in Nitra, Tr. A. Hlinku 2, 949 76 Nitra, Slovak Republic, tel.: +421 37 6414 300, fax: +421 37 7417 003, e-mail: Stanislav.Zeman@uniag.sk

Acta technologica agriculturae 4
Nitra, Slovaca Universitas Agriculturae Nitriae, 2011, s. 98–101

SEPARATED SLURRY BEDDING AND ITS EXPLOITATION IN LYING CUBICLES FOR DAIRY CATTLE

SEPAROVANÝ KAL HNOJOVICE A JEHO VYUŽITIE PRE PODSTIELANIE LEŽISKOVÝCH BOXOV DOJNÍC

Jana LENDELOVÁ,¹ Ľubomír BOTTO,² Vojtech BRESTENSKÝ²

Slovak University of Agriculture in Nitra, Slovak Republic¹
Animal Production Research Centre Nitra, Lužianky, Slovak Republic²

This paper deals with evaluating in 2 stables the exploitation of lying cubicles for housing dairy cows littered with separated slurry. There were 86 lying cubicles evaluated in the stable “V” and 87 lying cubicles in the stable “T”. In both stables, cows were milked in the morning and in the evening, separated by an approximate interval of 12 hours. The exploitation of lying cubicles was evaluated on the basis of monitoring daily behaviour of cows by identical researchers who performed a direct observation at an interval of 10 minutes. The following behaviour was observed: normal lying with cow’s head situated near the brisket locator (L), contrary lying with cow’s head situated near the rear curb (Lo), standing with 2 front legs in the lying cubicle (Sf), and standing with 4 legs in the lying cubicle (S). Furthermore, lying in alleys (La), standing in alleys (Sa), movement in alleys (M), feeding (F) and drinking (D) were also evaluated. In the stable “V”, cows were lying in cubicles in their natural position (L) 33.13 % of the time out of the 12 hour daily observation (it was 31.08 % for the stable “T”). The total time which cows spent in cubicles by lying or standing (L + Lo + Sf + S) was 40.98 % in the stable “V” and 56.86 % in the stable “T”. In the stable “T”, cows used to lie down into wet alleys 5 times more frequently than in the stable “V”, and the total time of lying in individual cubicles was significantly affected by direct solar radiation not accepted by animals.

Key words: bedding, separated slurry, lying, dairy cows

Behaviour is an indicator of animal welfare; animals respond sensitively through their individual behavioural expressions, such as lying, standing, feeding, movement, drinking, etc., to the parameters of the breeding environment influencing their comfort. First of all, the time spent by lying, the lying frequency and the lying length are considered a sensitive rate of comfort in the housing area (Haley *et al.*, 2000). According to a number of experts, lying as a welfare parameter has a higher priority than feeding and social contact when the opportunity to express behaviour is limited (Munksgaard *et al.*, 2005). The lying frequency and time spent by lying during 24 hours are used as indicators of animal comfort. Animal behaviour related to resting in lying areas in a loose housing system is influenced by constructional factors of the stable and its operating mode. The most important factors are the surface properties of flooring and the quality of bedding (Fregonessi *et al.*, 2007), stable orientation and internal layout (Wagner-Storch *et al.*, 2003), as well as the housing area per animal. The objective of this work was to evaluate in 2 stables the exploitation of lying cubicles for dairy cows littered with separated slurry and separated digested sludge, as this modified bedding material is progressively substituting the straw bedding that is more exacting in terms of operation and cost.

Materials and methods

The evaluation was performed in 2 dairy farms. The first one used as a bedding a separated digested sludge from the biogas station (stable “V”), and, in the second one, there was a directly separated and thermally treated slurry without prior digestion (stable “T”). The stables are situated in similar climatic

conditions, at a mutual distance of 20 km, and there were approximately identical weather conditions in examined days. In the stable “V”, there were evaluated 86 dairy cows housed in deepened lying cubicles arranged in two rows, with a central dunging passage 3.2 m wide and with an external feeding. Lying cubicles were 1 200 mm wide and 2 400 mm long, with a 300 mm – high rear curb, and the concrete brisket board delimited the area for lying in the position of 1 900 mm from the entry edge of the cubicle and exceeded the passage level by 400 mm. The diagonal distance from the rear curb edge to a neck rail was 1 985 mm. The milking process was performed in a dovetail milking parlour (2 × 12) at 7.00 a.m. and at 7.00 p.m. During milking (absence of dairy cows), the rear cubicle part was checked, and the polluted bedding (with urine and excrements) was removed manually by throwing over into the dunging passage. The bedding material was filled up to the curb level as necessary. Passage ways were cleaned using an automatic blade at 2 hour intervals. Heat stress in the summer period was eliminated using 8 fans with a diameter of 910 mm and power of 21 200 m³.h⁻¹. In the stable “T”, 176 dairy cows were housed in lying cubicles 1 200 mm wide and 2 500 mm long, with a 250 mm – high rear curb. In front of the concrete brisket board, a plastic pipe barrier was installed in order to allocate animals stricter during lying and standing in the cubicle. The diagonal distance from the rear curb edge to the neck rail was 1 950 mm. Animals were milked in the dovetail milking parlour (2 × 10) between 4.00 a.m. and 6.00 a.m. in the morning and between 4.00 p.m. and 6.00 p.m. in the afternoon. There were 87 dairy cows observed and divided into 2 groups with 44 and 43 animals. Showers were activated in the first group and fans in the second group. Alleys were cleaned using the automatic blade at 2 hour intervals. Cubicle exploitation was evaluated on the basis of monitoring daily behaviour of

dairy cattle upon direct observation by identical researchers at 10 minute intervals. The following behaviour was observed: normal lying with cow's head situated near the brisket locator (L), contrary lying with cow's head situated near the rear curb (Lo), standing with 2 front legs in the cubicle (Sf), and standing with 4 legs in the cubicle (S). Furthermore, lying in alleys (La), standing in alleys (Sa), movement in alleys (M), feeding (F) and drinking (D) were also evaluated. The evaluation was carried out between 2 milkings under daily light in the buildings during 12 hours. Ethograms enabled to evaluate the total time of animal behaviour, partial expressions at hourly intervals, and the exploitation of lying cubicles by dairy cows.

Results and discussion

In the stable "V", cows were lying in cubicles in their natural position (L) 33.13 % of the time out of the evaluated daily behaviour during 12 hours. The total time which cows spent in cubicles by lying or standing (L + Lo + Sf + S) reached 40.97 % in the stable "V".

However, contrary lying with cow's head situated near the rear curb (Lo) makes the smallest part of the investigated period. A greater part was represented by standing with 2 front legs (Sf) in the cubicle (6.27 %) or standing (S) with 4 legs in the cubicle (1.38 %). The whole lying time was 33.13 %. Contrary lying (Lo), the consequence of which is high cubicle soiling, makes 0.19 % of the time and it occurred only in 3 cubicles with a released cubicle width to 1 350 – 1 400 mm. Lying in alleys (La) associated with a significant soiling of udder and belly took only 0.53 % of the time. Standing with 2 front legs (Sf) and standing with 4 legs in the cubicle represented nearly one fifth of the cubicle occupation time (out of 40.97 % – lying, contrary lying, standing and standing by 2 front legs in total). It is the time when animal claws have a rest from direct contact with the wet soiled floor. Probably, also cross ventilation played a notable role because its straight flow was intensive for animals while

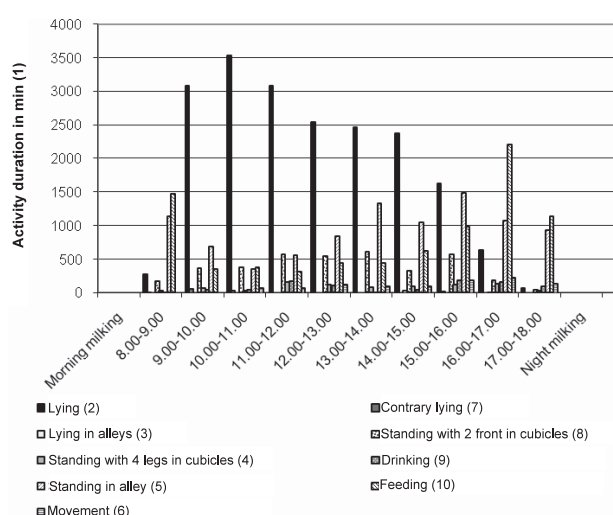


Figure 1 Behavioural expressions observed at hourly intervals between the morning and evening milking in the stable "V"

Obrázok 1 Sledované prejavy správania v hodinových intervaloch medzi raňajším a večerným dojením v objekte „V“
(1) trvanie aktivity v min, (2) ležanie v boxe, (3) ležanie v chodbách, (4) státie 4 nohami v boxoch, (5) státie v chodbe, (6) pohyb, (7) opačné ležanie, (8) státie 2 prednými nohami v boxoch, (9) pitie, (10) žranie

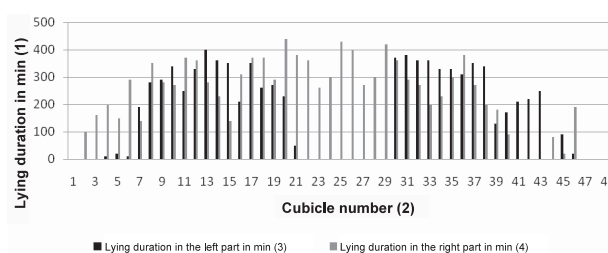


Figure 2 Scheme of utilisation of individual cubicles as natural lying ("L") in the stable "V"

Obrázok 2 Schéma využívania jednotlivých boxov formou prirodzeného ležania („L“) v objekte „V“
(1) doba ležania v min, (2) číslo boxu, (3) trvanie ležania v ľavej časti v min, (4) trvanie ležania v pravej časti v min

being in the standing position. The time course of individual daily behavioural expressions in cows is shown in Figure 1.

During monitoring the stable "V", especially in the period between 2 milkings (in the morning and in the evening), that is, during the day, the occupation of cubicles with the bedding of digested sludge from the biogas station amounted to 55.15 %.

It is evident from the analysis of exploitation of individual cubicles in relation to their position that the cubicles located at the entrance near the watering place were used only minimally (Figure 2). It is necessary to mention that a drinker was protected by no barrier, and the lying places were moistened on a number of occasions, or they were occupied by dairy cows in order to substitute access to the drinker.

It seems that animals perceive this disturbance and moisture and they are searching for calmer places. The lying cubicles situated opposite the drinkers were regularly occupied. The most preferred cubicles were occupied from 380 minutes to 440 minutes (6.33 – 7.33 hours). They were cubicles No 13, 14 and 15 in the right row and No 20, 21 and 22 in the left row in the front half of the stable. In the back half of the stable, they were cubicles No 33 – 38 in the right row and No 26, 29 and 30 in the left row. The outermost 6 – 8 cubicles were generally exploited less than 50 % of the time; some cubicles at the end were not used during the day at all. The length of lying can be influenced not only by the quality of the resting area but also by a closer harmonisation of operating actions with a daily regime of animals. Reserves occurred, for example in a late littering and cleaning of cubicles, after the return of animals from the milking parlour and their feeding, or if the feeding machine came to the group of cows too early – before milking. It is the time when animals would probably like to rest, but the sound of the feeding machine is an impulse for leaving the resting area and moving to the feeding manger, shortening the lying time. During monitoring cows' behaviour in the stable "T", it was found that animals were lying in cubicles 34.07 % of the observed 12 hour daily period. The time of milking had a minor effect (Figure 4 on the left). The total time spent in the cubicle (L + Lo + Sf + S) represented 61.33 % of the net stay of animals in the stable between milkings. Also this stable revealed similar circumstances, such as a late bedding process and feeding during the resting time. The lying time could be affected by evaporative cooling and fans; the outermost cubicle row in the first group was dazzled by the sunlight in the morning, and the outermost row in the second group was dazzled by the sunlight in the afternoon, but a moderate increasing of local air circulation traditionally in the afternoon made it possible to remove excess heat from animals.

The distribution of examined behavioural expressions in the stable "T" during 12 hours is shown in Figure 3.

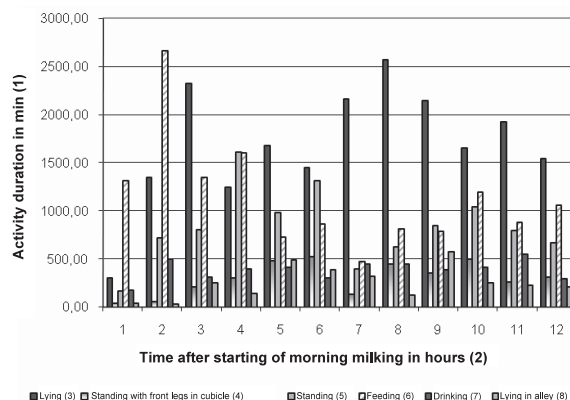


Figure 3 Behavioural expressions observed at hourly intervals between the morning and afternoon milking in the stable "T"
Obrázok 3 Sledované prejavy správania v hodinových intervaloch medzi raňajším a večerným dojením v objekte „T“
 Trvanie aktivity, min, (2) čas meraný od začiatku raňajšieho dojenia v h, (3) ležanie v boxe, (4) státie 2 prednými nohami v boxe, (5) státie v chodbe, (6) žranie, (7) pitie, (8) ležanie v chodbách

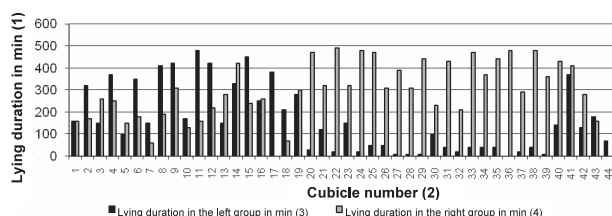


Figure 4 Scheme of utilisation of individual cubicles as natural lying ("L") in the stable "T" between 2 milkings
Obrázok 4 Schéma využívania jednotlivých boxov formou prirodzeného ležania („L“) v objekte „T“ medzi raňajším a večerným dojením
 (1) doba ležania v min, (2) číslo boxu, (3) trvanie ležania v ľavej skupine v min, (4) trvanie ležania v pravej skupine v min

The most visited lying cubicles in the stable "T" were occupied during the day for 430 – 490 minutes (7.1 – 8.1 hours). There were used mainly cubicles No 19 – 43 in the right group situated in the outermost row near the opened wall. However, the cubicles in the rear row were not used in preference but they belonged to the above-average exploited cubicles (but in this case, the end cubicles were separated by wooden barriers eliminating side excitement). Before noon, cows avoided dazzled cubicles No 20 – 44 in the outermost row of the east-oriented left group. In this time, they preferred cubicles No 1 – 19 situated in the internal row (Figure 4).

The total lying time in the cubicles and alleys of the stable "T" took 39.2 % of the monitored time. Contrary lying with cow's head situated near the rear curb (Lo) was not found in this stable. However, animals were lying in the dunging passage 5 times more than in the stable "V".

Feeding, drinking and milking together represented a smaller part in the stable "V", but a great part of feeding was performed before the morning milking. The area near the drinkers was often occupied in the stable "V", but presence at this place was not always for the purpose of drinking. This place was a free area often with an increased flow of fresh air, and animals stayed there only standing. Separated sludge in the form of "plastic bedding" offers a bedding material comparable with straw. It is possible to predict only a little soiling of animals on a small body area, increased only by 6 % in comparison with the straw bedding material (Šoch, 2005). The work focused on studying the occupation of cubicles bedded with separated sludge that can be

affected by other factors as well. Drissler et al. (2005) found that for every 1 cm decrease in bedding, cows spent 11 minutes less time lying down during each 24 hour period. Therefore, it is necessary to ensure in such cubicles a periodical refilling and supplies of a sufficient amount of bedding material. An incorrect position of the neck rail can cause problems with the lying down process – mainly to big animals (Bickert et al., 2000; Haley et al., 2000). The time of lying is shortened, and the time of standing is prolonged in this way, having an unfavourable impact on the health condition of legs. Also a very high brisket board or its placement very closely to rear curbs invokes concerns in animals regarding lying down (Tucker et al., 2006).

Conclusions

The monitoring of behavioural expressions in dairy cows, which were housed in stables with lying cubicles bedded with separated digested sludge or separated slurry, showed that there did not occur any deterioration of results in any of the observed parameters compared with the previous classical bedding material – straw. There were satisfactory results of breeders as far as the somatic cell counts, milking capacity and the total health condition in animals were concerned.

A detailed cubicle monitoring enabled to find other facts that besides the bedding material influenced the total lying time evidently. The most striking fact in the stable "V" was disharmony in working operations (food and bed filling at night during a possible resting time) and the lying of animals in the dunging passage in the stable "T", as well as direct solar radiation into the lying area in the outermost rows of cubicles.

The bedding material itself was well-accepted by animals, and the consequential analyses of odour level and concentration of emissions were below one third of critical values. The following issue remains open: temperature modifications in the thermic process of this bedding material with an emphasis on absolute exclusion of bacteriological growing. However, the straw is a biologically active bedding too and brings the same bacteriological problem.

Súhrn

Hodnotilo sa využívanie ležiskových boxov v dvoch objektoch pre ustajnenie dojníc, ktoré boli podstielané separovaným kalom hnojovice. V objekte „V“ sa hodnotilo 86 ležiskových boxov, v objekte „T“ 87. V oboch objektoch prebiehalo raňajšie a večerné dojenie približne s 12 hodinovým časovým odstupom. Využívanie boxov bolo v oboch objektoch hodnotené na základe denného sledovania správania dojníc priamym pozorovaním v 10 minútových intervaloch identickými osobami. Z prejavov správania sa sledovalo ležanie v boxe hlavou pri hrudnej zábrane (L), ležanie v boxe opačne s hlavou pri stielivovom prahu (Lo), státie prednými nohami v boxe (Sp) a státie všetkými 4 nohami v boxe (S). Ďalej bolo sledované ležanie v chodbách (Lch), státie v chodbách (Sch), pohyb v chodbách (C), žranie (Ž) a pitie (P). V objekte „V“ dojnice v boxoch v prirodzenej polohe ležali (L) 33,13 % času z 12 hodinovej dennej doby sledovania, v objekte „T“ 31,08 % času. Celkový čas strávený v boxe zahŕňajúci ležanie a státie v boxe (L + Lo + Sp + S) predstavoval v objekte „V“ spolu 40,98 % času, v objekte „T“ až 56,86 % času. V objekte „T“ dojnice viac ako päťnásobne častejšie líhali do priestorov hnojnej chodby v porovnaní s objektom „V“ a celkový čas ležania v jednotlivých boxoch významne ovplyvnilo priame slnečné žiarenie, ktoré zvieratá neakceptovali.

Kľúčové slová: podstielka, separovaný kal, ležanie, dojnice

Acknowledgement

This paper was prepared with the support of VEGA project 1/0771/09.

References

- BICKERT, W. G. – HOLMES, B. – JANNI, K. – KAMMEL, D. – STOPWEL, R. – ZULOVICH, J. 2000. Dairy Freestall Housing and Equipment, MWPS-7, Seventh Edition, MidWest Plan Service, Iowa State University, Ames, Iowa.
- DRISLER, M. – GAWORSKI, M. – TUCKER, C. B. – WEARY, D. M. 2005. Freestall Maintenance: Effects on Lying Behavior of Dairy Cattle. In: Journal of Dairy Science, vol. 88, 2005, no. 7, p. 2381 – 2387.
- FREGONESI, J. A. – TUCKER, C. B. – WEARY, D. M. 2007. Overstocking reduces lying time in dairy cows. In: Journal of Dairy Science, 2007, no. 90, p. 3349 – 3354.
- HALEY, D. B. – RUSHEN, J. – DE PASSILLI, A. M. 2000. Behavioral indicators of cow comfort: Activity and resting behaviour of dairy cows in two types of housing. In: Canadian Journal of Animal Science, 2007, no. 80, p. 257 – 263.

- MUNSKGAARD, L. – JENSEN, M. B. – PEDERSEN, L. J. – HANSEN, S. W. – MATTHEWS, L. 2005. Quantifying behavioural priorities-effects of time constraints on behavior of dairy cows. In: Applied Animal Behavior Science, 2005, no. 92, p. 3 – 14.
- ŠOCH, M. 2005. Effect of environment on selected indices of cattle welfare. Scientific monograph. Faculty of Agriculture – University of South Bohemia, České Budějovice, 2005, 288 p.
- TUCKER, C. B. – ZDANOWICZ, G. – WEARY, D. M. 2006. Brisket Boards Reduce Freestall Use. In: Journal of Dairy Science, vol. 89, 2006, no. 7, p. 2603 – 2607.
- WAGNER-STORCH, A. M. – PALMER, R. W. – KAMMEL, D. W. 2003. Factors affecting stall use for different freestall bases. In: Journal of Dairy Science, 2003, no. 86, p. 2253 – 2266.

Contact address:

Ing. Jana Lendelová, PhD., Department of Structures, Faculty of Engineering, Slovak University of Agriculture in Nitra, Tr. A. Hlinku 2, 949 76 Nitra, Slovakia, e-mail: Jana.Lendelova@uniag.sk

Acta technologica agriculturae 4
Nitra, Slovaca Universitas Agriculturae Nitriae, 2011, s. 101–104

EQUILIBRIUM MOISTURE OF CEREAL GRAINS

ROVNOVÁŽNA VLNKOSŤ ZŔN OBILNÍN

Ivan VITÁZEK, Juraj HAVELKA

Slovak University of Agriculture in Nitra, Slovakia

The drying process of agricultural products is divided in two sections: the section of permanent rate of drying and the section of falling rate of drying. Considering the section of falling rate of drying, the equilibrium moisture is decreased. Using the Henderson's relation for the equilibrium moisture of wet air the authors proposed a completed i-x-w diagram of wet air and given material with a graphic representation of equilibrium moisture of the given material within the whole presented area of unsaturated wet air for wheat, rye, barley and oats. Such approach enables to perform a more precise evaluation of the drying process and modelling of the process using the thermodynamic relations of wet air.

Key words: equilibrium moisture, cereal grains, diagram of wet air, linear regression

A majority of agricultural products, such as cereal grains, hay and forage, are harvested with relatively high moisture content and must be dried to reach the most advantageous (standard) moisture content which enables a long-term storage.

The heated atmospheric air is the most used drying medium. The end part of the drying process passes within the area of unsaturated wet air where the dried material is in the limit state of the equilibrium moisture content.

Changes in the atmospheric air states during the drying process are solved using the thermodynamics of wet air presented by a visual diagram of wet air (Chyský, 1977).

Equilibrium moisture contents are available only in several table values or sorption isotherms for one temperature only, as a result of a laboratory research. Such information is insufficient for practical purposes. Therefore, the authors developed a new method for the presentation of equilibrium moisture contents in the i-x diagram of wet air. It is called by the authors as the i-x-w

diagram of wet air and equilibrium moisture contents of the given material. This i-x-w diagram enables a more precise solution of the drying process in the falling rate section and the evaluation of the state of stored dried materials.

Materials and methods

Used definitions

Relative humidity of wet air φ is given by a ratio between partial vapour pressure in this air p_p and saturated vapour pressure p^* (from tables) at the same temperature:

$$\varphi = \frac{p_p}{p^*} \quad (1)$$

The relative humidity of saturated air is $\varphi = 1$ (100 %). The relative humidity of unsaturated air is less than 1 (less than 100 %).

Moisture content dry basis u of the material is given by a ratio between humidity mass in this material M_w and dry part mass in this material M_{MS} :

$$u = \frac{M_w}{M_{MS}}, \text{ kg/kg} \quad (2)$$

Moisture content wet basis w of the material is given by a ratio between humidity mass in this material M_w and whole mass M_M of this material:

$$w = \frac{M_w}{M_M} \cdot 100 = 100 \cdot \frac{M_w}{M_{MS} + M_w}, \% \quad (3)$$

Mutual relationships of u and w are given by the relations:

$$w = \frac{100 \cdot u}{1 + u} \quad u = \frac{w}{100 - w} \quad (4, 5)$$

In practice, the moisture content wet basis w is used to express the humidity of a material. In the theory of thermodynamics of drying processes, it is the moisture content dry basis u .

The curve of drying (Figure 1) is a graphical representation of the course of moisture content dry basis u versus time τ . It is divided in two sections:

- **Section of permanent rate of drying** – it means the time period within which a surface evaporation of humidity prevails. Humidity behaves as a free water level.
- **Section of falling rate of drying** – it means the time period within which the decrease of humidity is not proportional to the time and, theoretically, it ends in infinity.
- **Critical point** means the point which separates the section of permanent rate of drying and the section of falling rate of drying.
- The process of drying within the section of falling rate of drying results in desorption of humidity.

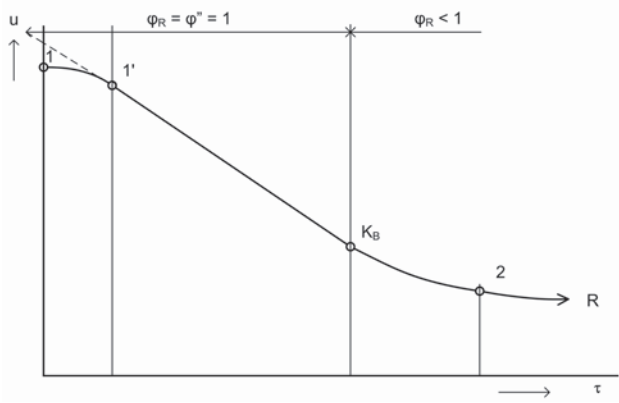


Figure 1 Curve of drying
1 – start of drying, 2 – end of drying, KB – critical point, R – point of equilibrium moisture which theoretically ends in infinity, 1 – 1' – section of increasing rate of drying, 1' – KB – section of permanent rate of drying, KB – R – section of falling rate of drying

Obrázok 1 Krivka sušenia
1 – začiatok sušenia, 2 – koniec sušenia, KB – kritický bod, R – rovnovážny bod, teoreticky v ∞ , 1 – 1' – úsek vzrastajúcej rýchlosti sušenia, 1' – KB – úsek stálnej rýchlosti sušenia, KB – R – úsek klesajúcej rýchlosti sušenia

Sorption isotherm (Figure 2) is a graphical representation of equilibrium moisture of the material w_r versus the relative humidity of ambient wet air φ_r at the given temperature t . In addition to the graphical description of sorption isotherms, we use representation with table values $w_r = f(\varphi_r)_{t=\text{const.}}$ and also an analytical representation using the equation $\varphi_r = f(t, u_r)$.

Equilibrium moisture is a moisture content (w_r, u_r) relevant to the state of thermodynamic equilibrium between the substance and ambient air.

Analytical equations for equilibrium moisture

In this work, the authors used the analytical equation of Henderson (1952) for the equilibrium moisture content:

$$1 - \varphi_r = \exp(-a \cdot T \cdot u_r^n) \quad (6)$$

where:

T – absolute temperature, K

u_r – moisture content dry basis, kg/kg

a, n – constants specific for each material

The authors transformed equation (6) for linear regression. They multiplied the first logarithm of equation (6) by -1:

$$-\ln(1 - \varphi_r) = a \cdot T \cdot u_r^n \quad (7)$$

The second logarithm of equation (7) is as follows:

$$\ln(-\ln(1 - \varphi_r)) = \ln a + \ln T + n \cdot \ln u_r \quad (8)$$

We use this equation for the linear regression of table values of equilibrium moisture contents dry basis of cereals from tables in (Pabis, 1982):

$$Y = A + B \cdot X \quad (9)$$

where:

$$Y = \ln(-\ln(1 - \varphi_r)) \quad (10)$$

$$A = \ln a + \ln T \quad (11)$$

$$X = \ln u_r = \ln \frac{w_r}{100 - w_r} \quad (12)$$

With the linear regression we obtain the values of A and B , of which we deduce:

$$n = B \quad (13)$$

$$a = \exp(A - \ln T) \quad (14)$$

Results and discussion

Equilibrium moisture content of cereal grains

Using the values presented in Pabis (1982) the authors took over the table values of equilibrium moisture content wet basis w_r for four sorts of cereal grains at temperature 20 °C, for the relative humidity of the air from 20 % to 90 %, for air pressure $p = 101.325$ kPa (Pabis did not provide these values).

These isotherms are presented in Figure 2 in coordinates w_r, φ_r .

Using the linear regression of equation (6) we obtained the Henderson's analytical equation for these materials:

$$\text{Wheat: } \varphi = 1 - \exp(-0.2053 \cdot T \cdot u_r^{2.2376}) \quad r = 0.994 \quad (15)$$

$$\text{Rye: } \varphi = 1 - \exp(-0.1602 \cdot T \cdot u_r^{2.1659}) \quad r = 0.9941 \quad (16)$$

$$\text{Barley: } \varphi = 1 - \exp(-0.1679 \cdot T \cdot u_r^{2.1862}) \quad r = 0.9943 \quad (17)$$

$$\text{Oats: } \varphi = 1 - \exp(-0.1126 \cdot T \cdot u_r^{1.8626}) \quad r = 0.9948 \quad (18)$$

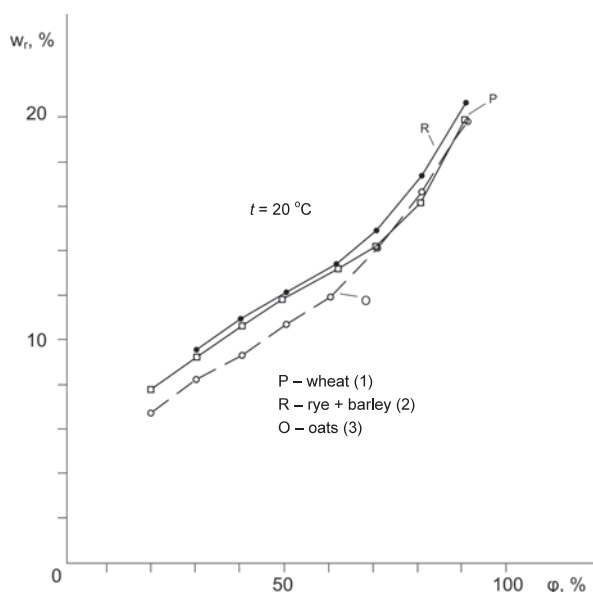


Figure 2 Sorption isotherms for four materials
Obrázok 2 Sorpčné izotermy pre štyri materiály
 (1) P – pšenica, (2) R – raž + jačmeň, (3) O – ovos

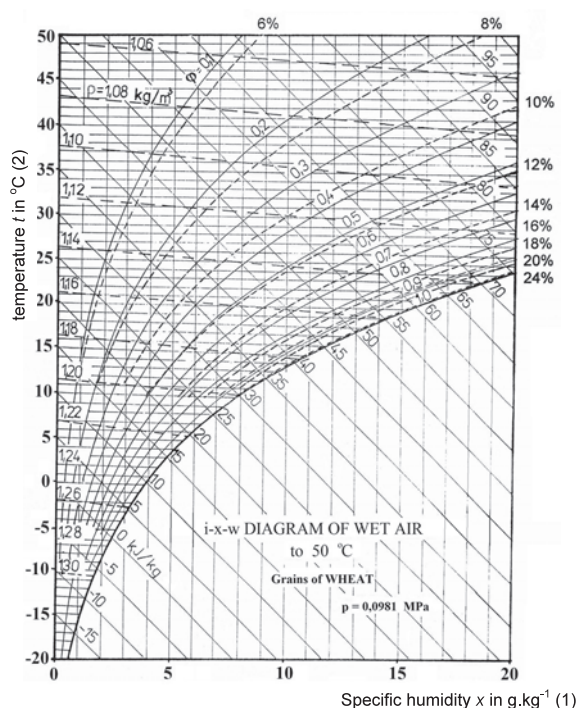


Figure 3 i-x-w diagram of wet air and grains of wheat
Obrázok 3 i-x-w diagram vlhkého vzduchu a zrn pšenice
 (1) merná vlhkosť vzduchu x v g.kg⁻¹, (2) teplota t v °C

The equations for rye and barley are nearly identical.

We used the constant values of a , n in equation (6) to calculate the courses of sorption isotherms in coordinates ϕ , t for the equilibrium moisture contents $w_r = 8\%$; 10% ; 12% ; 14% ; 16% ; 18% ; 20% ; 24% .

These curves $w_r = \text{const.}$ were plotted into the i-x diagram of wet air in coordinates ϕ , t .

Figures 3, 4 and 5 in the annex provide the i-x-w diagrams for wheat, rye, barley and oats.

Within the section of permanent rate of drying, where the relative moisture content of the material is higher than the moisture content in the critical point, the equilibrium moisture of all materials is equal to the relative humidity of saturated air $\phi^* = 1$.

Within the section of falling rate of drying, where the relative moisture content of the material is lower than its relative moisture content in the critical point, the equilibrium moisture content of the material is given by its sorption characteristics which depend on the kind of the material.

The contribution of the submitted paper is in the method which enables to obtain and transfer the values of equilibrium moisture content of the material into the i-x diagram of wet air within the whole range of the diagram.

A modified diagram for meadow hay was presented by Havelka (1973) and the i-x-w diagram for vegetable seeds was

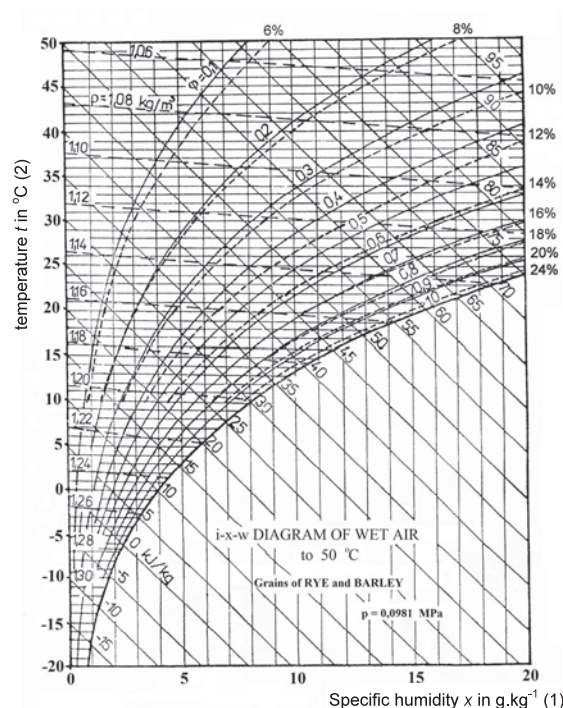


Figure 4 i-x-w diagram of wet air and grains of rye and barley
Obrázok 4 i-x-w diagram vlhkého vzduchu a zrn raže a jačmeňa
 (1) merná vlhkosť vzduchu x v g.kg⁻¹, (2) teplota t v °C

Table 1 Equilibrium moisture content wet basis w_r at temperature 20 °C

ϕ in %	20	30	40	50	60	70	80	90
Wheat (1)	7.80	9.24	10.68	11.84	13.10	14.30	16.02	19.95
Rye (2)	8.26	9.47	10.88	12.20	13.46	15.18	17.43	20.80
Barley (3)	8.25	9.50	10.90	12.00	13.40	15.20	17.49	20.50
Oats (4)	6.74	8.25	9.41	10.75	12.02	14.39	16.82	19.94

Tabuľka 1 Rovnovážne vlhkosti materiálov w_r pri teplote 20 °C
 (1) pšenica, (2) raž, (3) jačmeň, (4) ovos

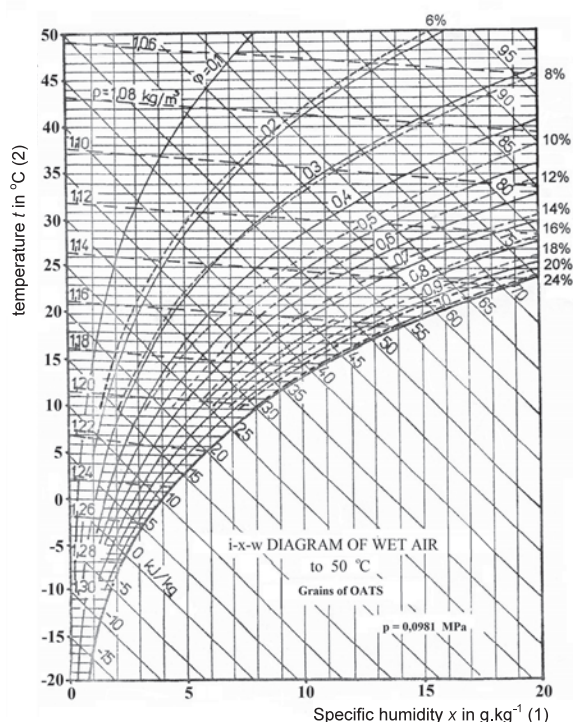


Figure 5 i-x-w diagram of wet air and grains of oats
Obrázok 5 i-x-w diagram vlhkého vzduchu a zrn ovsu
 (1) merná vlhkosť vzduchu x v g.kg^{-1} , (2) teplota t v $^{\circ}\text{C}$

presented by Vitázek (1996). Vitázek (2006) in his paper deals with a modification of i-x diagrams and its application.

Conclusions

The i-x-w diagram of wet air and the given humid material presents a new type of the diagram that we do not find in the bibliography. The user obtains an opportunity to get more detailed information about equilibrium moisture contents comparing to the table values of sorption isotherms.

These new diagrams enable to make a more precise modelling or evaluation of the process of drying. The authors used this approach successfully. Therefore, they will continue in their improvement.

Súhrn

Proces sušenia poľnohospodárskych materiálov tvorí úsek stálej rýchlosti sušenia a úsek klesajúcej rýchlosti sušenia. V úseku klesajúcej rýchlosti sušenia sa znižuje rovnovážna vlhkosť materiálu. Autori navrhli pomocou Hendersonovej rovnice pre rovnovážnu vlhkosť vzduchu doplnený i-x-w diagram vlhkého vzduchu a daného materiálu, v ktorom sú graficky znázornené rovnovážne relatívne vlhkosti daného zrna v celej znázornenej oblasti nenasýteného vzduchu pre pšenicu, raž, jačmeň a ovos. Umožní to dokonalejšie kontroly procesu sušenia a modelovanie procesu pomocou termodynamiky vlhkého vzduchu.

Kľúčové slová: rovnovážna vlhkosť, obilné zrná, diagram vlhkého vzduchu, lineárna regresia

Acknowledgement

This paper is prepared within the project VEGA 1/0708/09 "Research into the use of thermal energy from renewable resources in agricultural drying with respect to its impact on ecology and technology".

References

- HAVELKA, J. 1973. Optimalizácia sušenia sena s prihrievaním. In: Súčasná teória sušenia zrnovín a krmovín. Bratislava : DT SVTS, 1973, s. 229 - 238.
- HENDERSON, S. M. 1952. A Basic Concept of Equilibrium Moisture. In: Agricultural Engineering for January, 1952, p. 29 - 32.
- CHYSKÝ, J. 1977. Vlhký vzduch. Praha : SNTL, 1977, 161 s.
- PABIS, S. 1982. Teoria konwekcionogo suszenia produktow. Warszawa : PERiL, 1982, 229 p.
- VITÁZEK, I. 1996. Modifikovaný i-x diagram vlhkého. In: Poľnohospodárstvo, roč. 42, 1996, č 8, s. 645 - 651.
- VITÁZEK, I. 2006. Tepelné procesy v plynnom prostredí – Modifikované i-x diagramy. Nitra : SPU, 2006, 98 p. ISBN 80-8069-716-7.

Contact address:

doc. Ing. Ivan Vitázek, CSc., Slovak University of Agriculture in Nitra, Tr. A. Hlinku 2, 949 76 Nitra, Slovakia, phone: +421 37 641 47 56, e-mail: ivan.vitazek@uniag.sk

Acta technologica agriculturae 4
Nitra, Slovaca Universitas Agriculturae Nitriae, 2011, s. 105–109

IMPROVEMENT OF PROCESS PERFORMANCE AND EFFICIENCY IN A PRODUCTION ORGANISATION USING A SIX SIGMA METHOD

ZVYŠOVANIE VÝKONNOSTI A EFEKTÍVNOSTI PROCESOV VO VÝROBNEJ ORGANIZÁCII PROSTREDNÍCTVOM METÓDY SIX SIGMA

Maroš KORENKO, Pavol KAPLÍK

Slovak University of Agriculture in Nitra, Slovak Republic

Management methods for managing production processes and improving the quality of products should be part of every production organisation. Success in a competitive struggle for customers is always difficult for organisations, especially in times when global economy experiences recession. The reduction of undesirable variability, losses and costs associated with production processes can be achieved using the Six Sigma method. This method enables to increase the performance of processes and improve the quality of products. In this way, the organisation can achieve the compliance with customer's requirements imposed on the production holding more easily.

Key words: Six Sigma, production organisation, production quality

Recently, quality management has become a strategic issue in the top management of all customer-oriented organisations. Removing non-conformities after the production process is inefficient and financially much more expensive than prevention in the form of a quality management system. Therefore, it is important to analyse internal processes that leads to the disclosure of defects and hidden reserves for improving the functioning of the entire organisation (Savov and Džupina, 2007).

Pande (2000) defined Six Sigma as a comprehensive and flexible system for achieving, sustaining and maximising business success. Six Sigma is uniquely driven through a close understanding of customer's needs, disciplined use of facts, data and statistical analyses, and diligent attention to managing, improving and discovering business processes.

According to Keller (2005), Six Sigma programmes have many tools for improvement, including histograms, Pareto charts, statistical process control (SPC) and analysis of variance (ANOVA).

According to Pristavka (2009), an important group of statistical methods in engineering practice are analytical capabilities of instruments, production equipment and process capability. These quality tools are an active part in the application, development and continuous improvement of quality system efficiency. The investigation of process capability is the most commonly used from the above-mentioned statistical methods. The term "process capability" means the ability of the process to meet the specifications required by the specified value and tolerance limits. Bujna (2010) states that it is important to review the safety and risk process analysis and perform the hazard analysis. This analysis can be extended to the risks of the FMEA method. Possible measures to minimise risk are suggested after determining risk numbers.

According to Hrubec (2009), Six Sigma is a method of improving the quality, performance and efficiency of production. Improvement is performed through the organisation's own employees. Focusing on customers, processes and staff makes Six Sigma a way for building and developing a corporate culture (philosophy of Motorola).

According to Andrassyová (2010), quality improvement and new approaches to the monitoring and enhancement of quality standards is not completed. There is always a space for the optimisation of input data, production process and quality of a final product. This paper also forms an evidence of the statement and includes one of new approaches to the method studied.

Methods

Foster (2007) argued that a common approach to the implementation of improvement tools is a DMAIC methodology which is similar to the "plan of Edward Deming: Plan – Do – Check – Act" approach to solving problems. Lee-Mortimer (2006) considered the DMAIC methodology to be essential for Six Sigma programmes and adequate for providing business improvements. Holpp and Pande (2002) defined the Six Sigma process as follows:

1. Definition

Define essential resources that will require the clarification of search results, validation of the value (importance), establishment of borders and resources, communication plans and objectives, and identifying customers and their needs.

2. Measurement

Collect data to verify and quantify the problem, focus on priority setting and good decision on what criteria are needed.

3. Analysis

Find reasons to search through details, increase the understanding of the process and issue, and identify the culprit for the problem.

4. Improvement

Develop solutions and reduce problems, verify and confirm optimum solutions.

5. Control

Ensure a long-term impact on the way people work by promoting the development of the monitoring process, track changes that have been established and create response plans for solutions to problems that may arise.

Procedure: The basic procedure is based on DMAIC (Define, Measure, Analyse, Improve, Control)

1. Definition of products and services that the organisation intends to provide.

What is important for the customer? What is important for the organisation?

- Identifying the main opportunities.
- Awarding of the project.
- Setting goals.
- Identifying the sponsor and project team leader.
- Forming a team.
- Understanding of customer's requirements.

2. Measurement

What is the current level of performance of the organisation, its processes and products?

- Description and analysis of the current process performance.
- Verify and confirm the project objectives.
- Initial measurement.

3. Analysing

- Know the interrelationship between the inputs and outputs of processes.
- Determine the character of process performance.
- Identify sources and causes of variance and bottlenecks.
- Main types of losses.

4. Improving

- Generation of proposals.
- Testing of proposed solutions.
- Evaluate the impacts on the capacity and performance of processes.
- Action Plan implementation.
- Full implementation of proven solutions.

5. Management

- Documenting the results.
- Measures to maintain the improvements.
- Disclosure and valuation of results.

In various stages of DMAIC, the following related tools and methods are appropriately applied:

D – standard form, cost-benefit analysis, IPO diagram, FMEA (Failure Mode and Effect Analysis).

M – process map (definition and process modelling), cause and effect diagram (Ishikawa diagram), analysis of process inputs, histogram, Pareto analysis, process control chart, process capability analysis, FMEA.

A – cause and effect diagram (Ishikawa diagram), process capability analysis, process control chart, regression analysis, time characteristics of the process, analysis of bottlenecks, FMEA.

I – brainstorming, lean manufacturing tools, FMEA, graphical analysis, statistical analysis.

C – Poka Yoke, documented procedure for the operation, FMEA, control sheet, histogram (Hrubec, 2009).

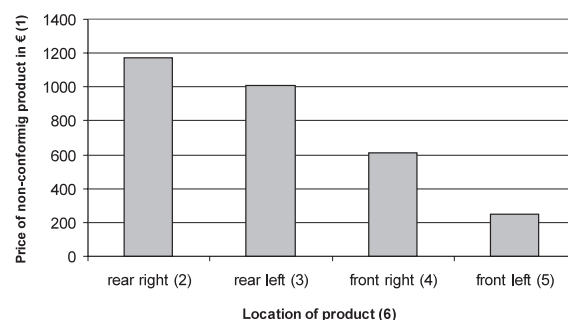


Figure 1 Losses caused by non-conforming products on the assembly line

Obrázok 1 Straty spôsobené nezhodnými výrobkami na montážnej linke (1) cena nezhodných výrobkov v €, (2) zadný pravý, (3) zadný ľavý, (4) predný pravý, (5) predný ľavý, (6) umiestnenie výrobku

implemented in the organisation (in the field of automotive industry) manufacturing door panels. Duration of project: from 24 August 2010 to 5 November 2010.

Definition

The main task is to reduce the cost of scraps from the assembly line. Therefore, it is necessary to specify the problem, solutions and the objective of solutions.

1. **The problem** is the lack of quality in door panels, while priority is to improve the quality of the rear parts of door panels.
2. **The solution area** is the assembly line because there occurs damage to the decorative strips of door panels and non-conforming products are made.
3. **The aim** is to reduce non-conforming products during the installation of decorative strips by at least 50 %.

Measurement

Measurements were performed after defining the problem. We specified the components most involved in material losses and causing major material damage. During the period of 24 August

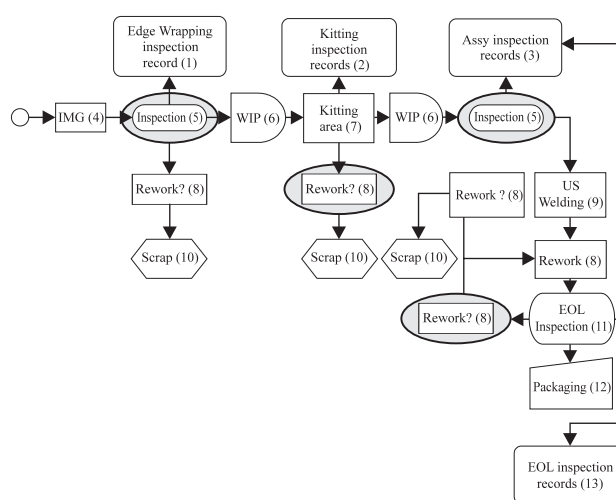


Figure 2 Process flow chart

Obrázok 2 Procesný diagram

(1) kontrolný záznam na vysekávačke, (2) inšpekčné záznamy pri príprave komponentov, (3) inšpekčné montážne záznamy, (4) potahovanie výlisku, (5) kontrola, (6) práca v procese, (7) príprava komponentov, (8) oprava, (9) zváranie, (10) nezhodný výrobok, (11) kontrola na výstupe, (12) balenie, (13) záznam z výstupnej kontroly

Results

Practical implementation of Six Sigma into the production process

The main objective of the project was the reduction of scraps on the assembly line by means of Six Sigma. The project was

2010 – 5 November 2010, 81 093 products were manufactured in total, of which 1 515 were non-conforming.

It is obvious that rear components represented the largest share in losses on the assembly line due to non-conforming products (Figure 1). Incurred non-conformities on manufactured products were of a decorative character (scratches, dents). Non-conformities on products were recorded in several places and entered in inspection records. The records consist of the following information: date, change, operator's name, type and location of non-conformity and working zone. This allows to analyse the process, the source field of errors, process influence on quality and the causes of non-conformity.

Figure 2 shows the process diagram of individual departments, material flows and places for collecting information. At the process input, extruded decorative strips and foil surface are covered with adhesive; in this way, they enter the machine to coat the plastic extrusion with a cover foil. A skin-like pattern is printed on the foil during coating (i.e. roughening). At the output, there are finished decorative strips mounted in door panels. If there are any problems found during the end-of-line inspection, non-conforming products are documented in assembly inspection records.

Analysis

At this stage, we have focused on tracking and naming non-conformities arising at individual workplaces. It is evident from Figures 3–6 that there is a difference in the occurrence of non-conformities at individual workplaces (some workplaces showing a higher while other a lower occurrence). Therefore, a

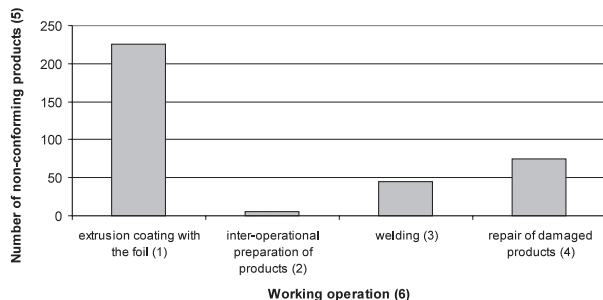


Figure 3 Non-conformity “impurity on the foil”
Obrázok 3 Chyba „nečistota na fólii”
(1) cena nezhodných výrobkov v €, (2) zadný pravý, (3) zadný ľavý, (4) predný pravý, (5) predný ľavý, (6) umiestnenie výrobku

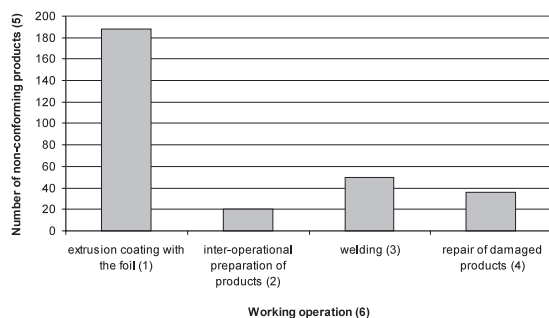


Figure 4 Non-conformity “damaged edge”
Obrázok 4 Nezhoda „poškodený roh”
(1) cena nezhodných výrobkov v €, (2) zadný pravý, (3) zadný ľavý, (4) predný pravý, (5) predný ľavý, (6) umiestnenie výrobku

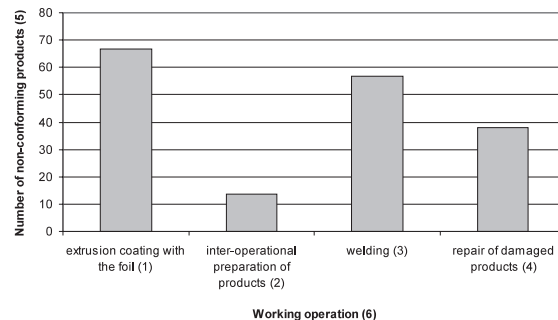


Figure 5 Non-conformity “damaged foil”
Obrázok 5 Nezhoda „poškodená fólia”
(1) cena nezhodných výrobkov v €, (2) zadný pravý, (3) zadný ľavý, (4) predný pravý, (5) predný ľavý, (6) umiestnenie výrobku

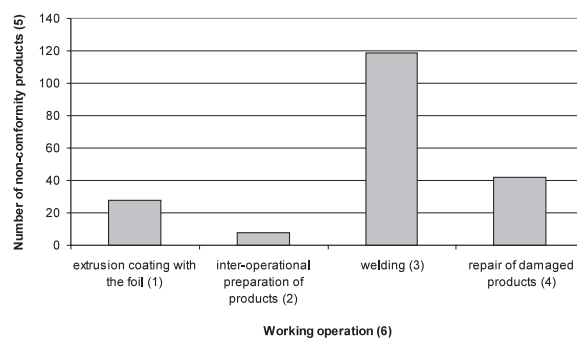


Figure 6 Non-conformity “hole in the foil”
Obrázok 6 Nezhoda „diera na fólii”
(1) cena nezhodných výrobkov v €, (2) zadný pravý, (3) zadný ľavý, (4) predný pravý, (5) predný ľavý, (6) umiestnenie výrobku

corrective measure will focus primarily on those workplaces where non-conformities on decorative strips occurred most, and we will propose measures that would eliminate the causes of their emergence.

Non-conformities from impurity on the foil occurred most frequently in the working operation “extrusion coating with the foil” and “repair of damaged products”.

The non-conformity “damaged edge” occurred most frequently in the working operation “extrusion coating with the foil” and “welding”.

The highest occurrence of the non-conformity “damaged foil” was recorded in the inspection of “extrusion coating with the foil” and “welding”.

We focused on the occurrence of the same non-conformity at individual workplaces. The fact that the non-conformity occurs at checkpoint No 1 means that it was generated before checkpoint No 1. If, for example, checkpoint No1 is “extrusion coating with the foil”, the non-conformity was created at the workplace “extrusion coating with the foil” or immediately before that workplace. If we did not record that non-compliance at checkpoint No 2 but it was recorded in an increased number at checkpoint No 3, the same non-conformity is generated immediately before checkpoint No 3. This means that the same kind of non-conformity is generated at two places, i.e. two different reasons for which it is necessary to identify two different corrective measures.

The non-conformity “hole in the foil” was recorded most in the working operation “welding” and “repair of damaged products”.

Improvement and management

After defining the most serious non-conformities making the greatest contributions to non-conforming products, and after identifying the most frequent places of their occurrence, we took corrective actions leading to the elimination of possible causes of defects in products.

We have defined non-conformities arising from impurities on the foil originated in the machine feeding the foil into the machine for extrusion coating. The corrective action to be taken is a periodic cleaning of guide rolls for coating the product with the foil in order to eliminate impurities (Figure 7).

Another corrective measure during the packaging of products after welding was the removal of a metal barrier (Figure 8) as a mutual contact between the barrier and product is a possible cause of damage to the product.

Further deterioration occurred in handling the package. Components were hung up to smooth metal hangers which made them close to each other, and any collision between them caused non-conformity, such as "damaged foil" and "hole in the foil".

Therefore, a corrective action was taken – smooth metal hangers were replaced by plastic hangers (notched). That enabled to hang the products at a distance and, thus, to prevent their mutual contact in handling the stands (Figure 9).

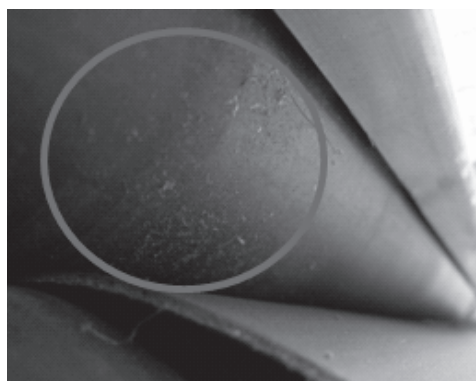


Figure 7 Impurity on guide rolls
Obrázok 7 Nečistota na vodičoch

Metal supports on punching machines, where the excess foil is trimmed from coated components, are a possible reason for errors because they are very hard and their surface is too smooth. A regular cleaning of metal supports from impurities was introduced.

Savings

Table 1 contains the numbers and prices of products on the assembly line before and after the implementation of corrective

Table 1 Price of non-conforming products before and after corrective actions

November 2010 – after the corrective action (1)							August 2010 – before the corrective action (3)					
Results from daily reports (2)							Results from daily reports (2)					
Date (4)	Number of manufactured products in pcs (5)	Number of non-conforming products in pcs (6)	Value of non-conforming products in € (7)	Number of non-conforming strips, pcs (8)	Price of non-conforming strips in € (9)		Date (4)	Number of manufactured products in pcs (5)	Number of non-conforming products in pcs (6)	Value of non-conforming products in € (7)	Number of non-conforming strips, pcs (8)	Price of non-conforming strips in € (9)
5. 11.	2 424	9	340	33	289		4. 8.	1 917				
6. 11.	2 164	15	567	13	114		5. 8.	3 191				
9. 11.	2 561	15	567	11	96		6. 8.	3 141				
10. 11.	1 518	8	302	0	0		7. 8.	2 797				
11. 11.	2 492	23	869	15	131		10. 8.	2 263				
12. 11.	2 375	10	378	19	166		11. 8.	1 638				
13. 11.	1 994	5	189	10	88		12. 8.	1 132				
16. 11.	2 657	7	265	14	123		13. 8.	2 280				
18. 11.	392	1	38	6	53		14. 8.	2 363				
19. 11.	2 649	5	189	12	105		17. 8.	3 023				
20. 11.	3 040	6	227	20	175		18. 8.	2 859				
Σ				153	1 139	difference	Σ			350	3 063	
% of door panels			0.63 %		0.69 %	% of door panels			1.32%			
€ per 1 door panel			0.06		0.06	€ per 1 door panel			0.12			
Number of cars produced per year (10)						160 000						
Number of door panels produced per year (11)						640 000						
Savings on strips, pcs (12)						4 416						
Scrap of strips (13)				35 309 €					73 673 €			
Savings on strips (14)				38 364 €								
Product price – 37.8 €,pc ⁻¹ (15)												
Strip price – 8.75 €,pc ⁻¹ (16)												

Tabuľka 1 Cena nezhodných výrobkov pred a po nápravných opatreniach

(1) november 2010 – po nápravnej akcii, (2) výsledky z denných správ, (3) august 2010 – pred nápravou akciou, (4) datum, (5) počet vyrobených výrobkov v ks, (6) počet nezhodných výrobkov v ks, (7) hodnota nezhodných výrobkov v €, (8) počet chybných páskov v ks, (9) cena chybných páskov v €, (10) počet vyrobených áut za rok, (11) počet vyrobených dverových panelov za rok, (12) úspora na páskoch v ks, (13) odpad na páskoch, (14) úspora na páskoch, (15) cena výrobku v €.ks⁻¹, (16) cena pásika v €.ks⁻¹

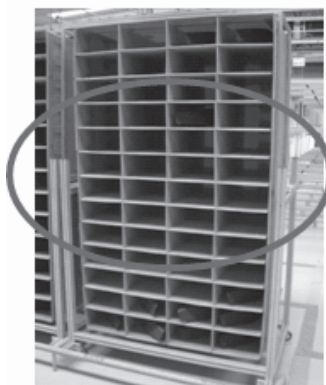


Figure 8 Packaging without the metal barrier
Obrázok 8 Balenie bez kovovej závery



Figure 9 Notched plastic hangers
Obrázok 9 Vrúbkované plastové vešiaky

measures. The comparison of a two-week production in August and two-week production in November provided an idea of reducing the number of non-conforming products on the assembly line.

Before corrective measures: 1.32 % – this number means that there were 1.32 pieces of non-conforming products on the assembly line per 100 pieces of produced door panels for the given reference period. This represented a loss of € 0.12 per 1 door panel made.

After corrective measures: 0.63 % – this number means that there were 0.63 pieces of non-conforming products on the assembly line per 100 pieces of produced door panels for the given reference period. This represented a loss of € 0.06 per 1 door panel made.

The production organisation produces 160 000 four-door cars annually and 640 000 door panels (1 car = 4 door panels). We have found that the saving on strips at the annual production of 640 000 door panels is 4 416 pieces amounting to € 38 364. These calculations show that the organisation can achieve said savings by improving performance and efficiency using the Six Sigma method.

Conclusions

The process of increasing the product quality and a continuous improvement of process performance belong to the key attributes that lead to successful production organisations and their ability to survive on the market.

This paper deals with the Six Sigma method that enables to achieve the continuous improvement of process performance and product quality. If the organisation wants to survive on the market and maintain its position in producing higher-quality products with lowest production losses, it must constantly

manage and improve its production processes. The fulfilment of customer's requirements and minimum production of non-conforming products create a path to the prosperity and growth of organisations. We address the reduction of non-conforming products in one of the components of door panels. A successful implementation of Six Sigma in production processes leads to the conclusion that the organisation may have reduced the annual losses of non-conforming products by more than 4 416 pieces representing a saving of approximately 38 364 €.

Súhrn

Manažérske metódy riadenia výrobných procesov a zlepšovanie kvality výrobkov by mali byť súčasťou azda každej výrobnjej organizácie. Obstať v konkurenčnom boji o zákazníka je pre organizácie vždy náročné, zvlášť v časoch, keď globálne hospodárstvo zažíva recesiú. Znižovanie nežiaducej variability, strát a nákladov spojených s výrobnými procesmi je možné dosiahnuť pomocou metódy Six Sigma. Touto metódou je možné dosiahnuť zvýšenie výkonnosti procesov a zlepšovanie kvality výrobkov. Organizácia tým môže ľahšie dosiahnuť splnenie požiadaviek, ktoré sú na výrobný podnik zo strany zákazníka kladené.

Kľúčové slová: Six Sigma, výrobná organizácia, kvalita výroby

This work was prepared within scientific research project VEGA 1/0576/09 "Improving the quality of agricultural machinery and production systems" conducted at the Department of Quality and Engineering Technologies, Faculty of Engineering, Slovak University of Agriculture in Nitra. In this way, we would like to thank to the management of Visteon Interiors Slovakia, s.r.o. for cooperation and disclosure of inside information.

References

- ANDRÁSSYOVÁ, Z. – KOTUS, M. 2010. Evaluation of CNC milling machine capability for transmission gear manufacturing. In: TRANSACTIONS of the VŠB – Technical University of Ostrava, Mechanical Series, vol. 56, no. 2, article no 1776. Ostrava : VŠB – TU, 2010. ISSN 1210-0471.
- FOSTER, S. T. 2007. Does Six Sigma Improve Performance? In: The Quality Management Journal, vol. 14, 2007, no. 4, p. 7 – 20. ISSN 1068-6967.
- HRUBEC, J. – VIRČÍKOVÁ, E. et al. 2009. Integrated Management System, 1 ed., Nitra : SPU, 2009, 543 p. ISBN 978-80-552-0231-0.
- Keller, P. 2005. Six Sigma: Demystified. McGraw-Hill, New York : NY, 2005, 427 p. ISBN 0-07-144544-7.
- PANDA, P. S. – NEUMAN, R. P. – CAVANAGH, R. R. 2000. The Six Sigma Way, McGraw-Hill, 2000, 422 p. ISBN 0-07-135806-4.
- CARPORTS, M. – HRUBEC, J. 2009. Capability of lathe-turning process of A points for gear box. In: Production Engineering, Novosibirsk State Technical University, 2009. ISBN 978-5-7782-1165-0.
- SAVOV, R. – DŽUPINA, M. 2007. Strategic Management in terms of quality businesses in Slovakia. In: Knowledge economy, trends in education, science and practice. Zlín : UTB, 2007. ISBN 978-80-7318-646-3.
- BUJNA, M. – KREDATÚSOVÁ, M. – BURDA, M. 2010. Identifikácia a analýza ohrozenia pre výrobný proces ložiska. In: Kvalita a spoľahlivosť technických systémov 2010, Sprievodná akcia medzinárodného strojárskeho veľtrhu 2010 v Nitre, Nitra : SPU, 2010, s. 95 – 99. ISBN 978-80-8069-890-4.

Contact address:

doc. Ing. Maroš Korenko, PhD., Ing. Pavol Kaplík, Slovak University of Agriculture in Nitra, Slovakia

Acta technologica agriculturae 4
Nitra, Slovaca Universitas Agriculturae Nitriae, 2011, s. 110–112

SURFACE WELDING OF SEEDBED CULTIVATOR SHARES WITH A SHIELDING GAS NAVÁRANIE RADLIČIEK KOMPAKTORA V OCHRANNEJ ATMOSFÉRE PLYNOV

Martin KOTUS,¹ Zuzana ANDRÁSSYOVÁ,¹ Ján ŽITŇANSKÝ,¹ Marián BUJNA,¹ Peter ŽÚBOR²

Slovak University of Agriculture in Nitra¹
In Weld Consulting, s.r.o. Trnava²

This contribution deals with evaluation of the shielding gas effect on abrasive wear in the surfacing of seedbed cultivator shares. In the determination of material resistance, the intensity of wear was monitored on the basis of mass and linear dimensions. The criterion of abrasion resistance is the relative resistance to abrasive wear and the HV 30 hardness of individual surfacing welds on the seedbed cultivator shares. The obtained results indicate that the use of shielding gases (especially the active, MAG) for the purpose of increasing abrasion resistance and thus prolonging the lifetime of the seedbed cultivator shares is very suitable.

Key words: seedbed cultivator shares, GMAW, abrasive wear, relative resistance

The working conditions of agricultural machinery adversely affect its lifetime and cause imbalances in the lifetime of nodes and functional parts of machinery. These problems cause downtime increasing, the necessity of repair interventions, or the purchase or replacement of damaged parts by spare parts.

The most common causes of failures in machine parts and structures are tribological processes on functional surfaces. As regards the avoidance of material losses, the most important task is attributed to the technologies of active material surface protection within friction nodes, for example renovation by surfacing (Viňáš, 2004).

In engineering practice, the resistance of materials to abrasive wear can be evaluated by measuring the dimensional changes and mass losses of worn parts or it can be assessed in relation to mechanical characteristics (e.g. hardness), the surface roughness of worn parts, etc. (Kotus et al., 2010; Paulíček et al., 2011).

The objective of this contribution was to verify the resistance of agricultural tools in working conditions with a predominant abrasive wear. The experiment was based on the surfacing of seedbed cultivator shares, to which a filler material was applied using the shielding gas.

Materials and methods

The filler material was applied to the duck-foot shares of the PB-6-022 seedbed cultivator. The base material of the shares was a steel of grade 12 051. Duck-foot shares are used for loosening the topsoil and for weed killing in the inter-rows of cultivated plants. They are used for the depths of 20 mm to 60 mm and the widths of 120 mm to 380 mm.

The seedbed cultivator shares were used in loam to clay loam soils in the south-eastern area of Nitrianska pahorkatina (hills) at an altitude of 155 m. Loam soils contain 30 % to 45 % of clay particles. Clay loam soils are bound to clay stones weathered easily and to heavier sediments with a low content of skeleton (Páltik et al., 2003).

Surfacing was performed using the Tiger 170 AC/DC inventor suitable for assembly and workshop operations. The

basic methods of surfacing were defined for the experiment; they were based on the methods of arc welding (GMAW – Gas Metal Arc Welding) using the inert or active shielding gas. When using the inert gas (argon), the given method is referred to as MIG (Metal Inert Gas), category 131 according to the Standard EN ISO 4063. When using the active gas (natural gas AGA MIX – 18 % CO₂), the given method is known as MAG (Metal Active Gas), category 135 according to the Standard EN ISO 4063.

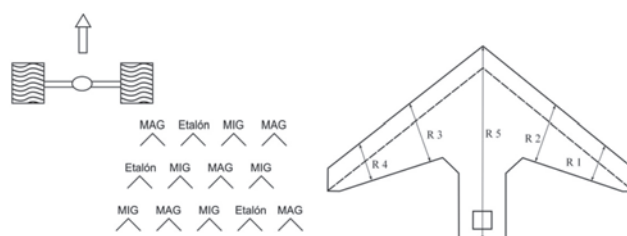


Figure 1 Location of the seedbed cultivator shares behind the tractor together with the measured planes (R1 – R5)

Obrázok 1 Umiestnenie radličiek kompaktora za traktor a roviny merania na radličke kompaktora (R1 – R5)

The alkaline tubular wire Welcaware 1736 with 1.2 mm in diameter and with chemical composition shown in Table 1 was used as the filler material. The given filler material is highly resistant to abrasive wear under medium stresses caused by shocks and pressure and is filled with the welding flux of metal powder. The surfacing weld is tough and homogeneous, yielding more than 80 % of the wire weight.

Table 1 Chemical composition of the filler material

Material (1)	Content of elements in % (2)					
	C	Mn	Si	Cr	Mo	Cu
Welcaware 1736	0.45	1.6	0.6	5.5	< 0.5	< 0.5

Tabuľka 1 Smerné chemické zloženie prídavného materiálu (1) materiál, (2) obsah prvkov v %

The tests of hardness were performed according to the Standard STN ISO 6507 (i.e. Vickers) with a load force of 294 N and using the HPO 250 device.

The relative resistance to abrasive wear is a basic criterion for material assessment; it was defined by the following adjusted Equation:

$$\Psi_{abr.} = \frac{W_{hE}}{W_h}$$

where:

W_{hE} – mass loss of etalons, g

W_h – mass loss of tested bodies, g

Surfacing together with the measurements of hardness, the changes in mass and in linear dimensions were performed by means of equipment and devices in the laboratories of the Department of Quality and Engineering Technologies (Faculty of Engineering, Slovak University of Agriculture in Nitra).

Results and discussion

The mass losses of individual duck-foot shares with respect to the location of fixing to the seedbed cultivator for the cultivation of 140 ha and 280 ha of the topsoil are shown in Figures 2 and 3. The graphic representation of the resistance of duck-foot shares is shown in relation to the shares without surfacing, the shares with surfacing in the inert gas (MIG) and the shares with surfacing in the active gas (MAG). Figure 4 shows the reduction of linear dimensions within the monitored planes for the cultivation of 280 ha of the topsoil.

It is possible to state on the basis of measured values that the mass losses for the active shielding gas (MAG) were lower than that observed with the inert gas (MIG) for all of the evaluated hectares of the cultivated soil. The highest level of wear was reached in the seedbed cultivator share (etalon) without surfacing, being confirmed by the highest measured mass and linear losses.

By comparing the values of losses of the seedbed cultivator shares in different rows, it is necessary to point out that the shares located directly behind the tractor wheel reached the highest level of wear. The share without surfacing was located

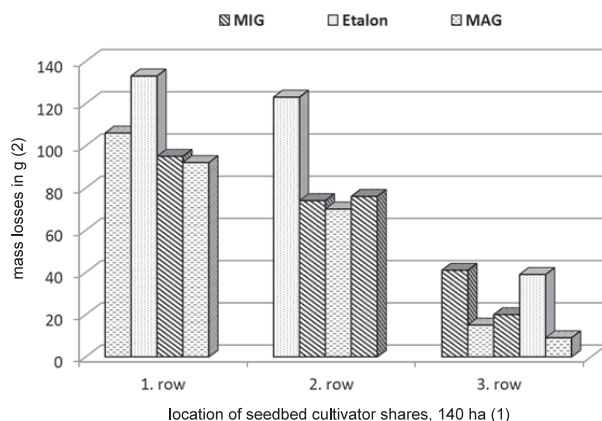


Figure 2 Mass losses of the seedbed cultivator shares for 140 ha of the cultivated soil

Obrazok 2 Úbytok hmotnosti radličiek pri opracovaní 140 ha pôdy (1) umiestnenie radličiek na kompaktore, 140 ha; (2) úbytok hmotnosti v g

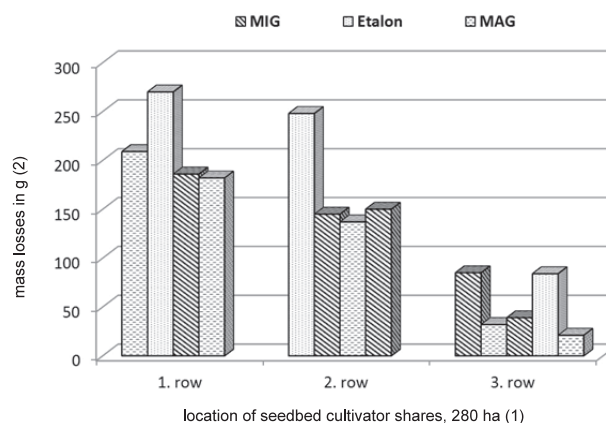


Figure 3 Mass losses of the seedbed cultivator shares for 280 ha of the cultivated soil

Obrazok 3 Úbytok hmotnosti radličiek pri opracovaní 280 ha pôdy (1) umiestnenie radličiek na kompaktore, 280 ha; (2) úbytok hmotnosti v g

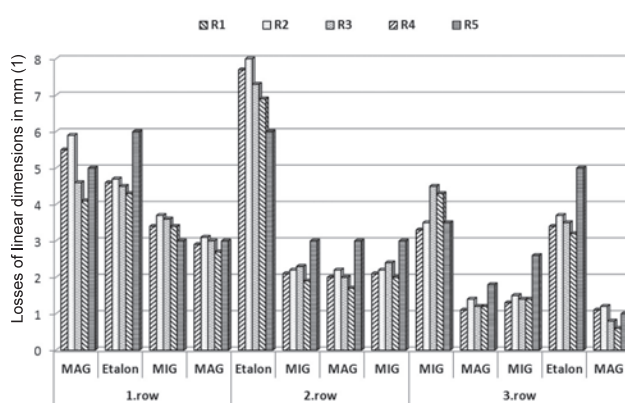


Figure 4 Reduction of linear dimensions of the seedbed cultivator shares for 280 ha of the cultivated soil

Obrazok 4 Úbytky lineárnych rozmerov radličiek pri opracovaní 280 ha pôdy (1) úbytok lineárnych rozmerov v mm

in the second row behind the tractor wheel. Almost two times higher level of wear was reached there as compared to the surfaced shares. In the third row, nearly the same losses were observed in the shares without surfacing and in the MIG-welded shares. The losses in mass and in linear dimensions were lowest in the shares located in the last row; this can be caused by a lower resistance of the soil mass to share penetration into the soil.

Figure 5 shows the graphical relationships of the HV 30 hardness measured in all of the shares before putting into operation. The reached hardness represents the average value of 5 measurements in the individual planes of measured linear dimensions. Calculated average values of the relative resistance to wear and HV 30 hardness in relation to the shielding gas are shown in Figure 6.

When comparing the shielding gases results, it is necessary to state that surfacing using the MAG method revealed an increase in the surfacing weld by 30 % as compared to the MIG method. That can be caused by different voltage during surfacing. Generally, surfacing in the argon shielding gas or by a mixture of gases rich of argon is considered to be regulated in a voltage higher by 4 V to 10 V. The width of the surfacing weld increases and its depth decreases with increasing the voltage during surfacing. These

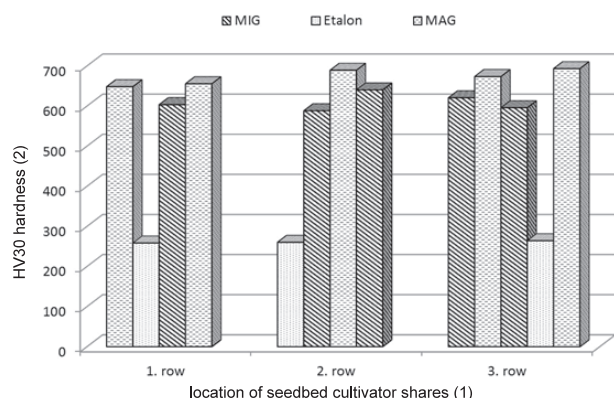


Figure 5 Values of the HV30 hardness of individual seedbed cultivator shares

Obrázok 5 Hodnoty tvrdosti HV30 jednotlivých radličiek kompaktora (1) umiestnenie radličiek na kompaktore, (2) tvrdosť HV30

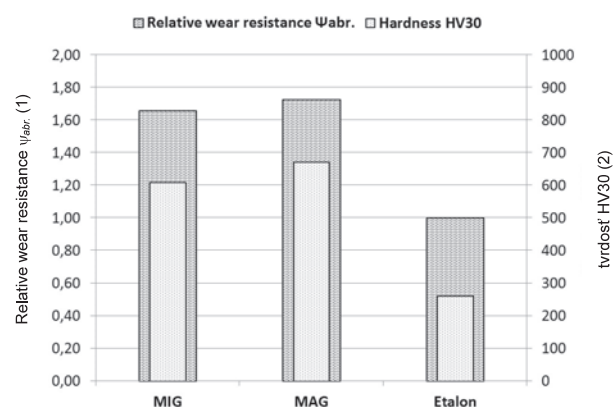


Figure 6 Average values of the relative resistance ψ_{abr} and HV30 hardness

Obrázok 6 Priemerné hodnoty pomernej odolnosti ψ_{abr} a tvrdosti HV30 (1) pomerná odolnosť ψ_{abr} , (2) tvrdosť HV30

parameters characterising the surfacing weld shape are crucial for the creation of abrasion resistant layers, which also determine the amount of the metal used.

This knowledge can influence the evaluation of abrasion resistance in the created layers. The results of measurements have confirmed higher resistance to wear in case of the shares made under the active gas. Also, the reached hardness was higher in the MAG-welded shares. That can be caused by less mixing between the filler and base material. The values of hardness in the shares without surfacing (260 HV30) were lower by half in comparison with the surfaced shares (610-670 HV30). At the same time, the relative resistance to wear was $\psi_{abr} = 1.66$ for the MIG method and $\psi_{abr} = 1.73$ in case of MAG.

Kovářková et al. (2011) reached the relative resistance to wear $\psi_{abr} = 3 \div 5$ in case of the NP 16, NP 22, NP 42, NP 62 metal powders with an admixture of wolfram carbides applied by a CO₂ laser. The structure of these surfacing welds is formed by the base matrix of nickel and austenite with the particles of wolfram carbides being present. In the heat-affected zone, there was a martensite layer and ferrite decarburisation layer.

Mikuš et al. (2006) used the NP 58 filler powder in their study; the surfacing weld was prepared on the base layer fixed to the soil cultivation tool. The filler powder was applied by the NPK-1 torch with an oxy-acetylene flame, and they reached the relative resistance to wear $\psi_{abr} = 1.23$.

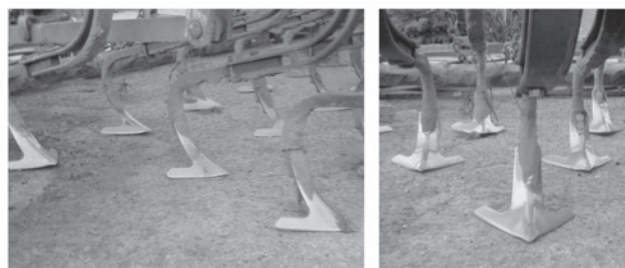


Figure 7 Wear of the seedbed cultivator shares after cultivation of 280 ha
Obrázok 7 Opotrebené radličky kompaktora po opracovaní 280 ha pôdy

Kovářková (2007) states that current filler materials are based on the alloying of Cr and C and thus obtaining a high amount of carbides of Cr in the surfacing welds and good resistance to abrasive wear. It must not be forgotten that the technologies of arc surfacing cause the releasing of carcinogenic chromium into the air, which causes damage to welder's health. Therefore, it is necessary to reduce the contents of the Cr particles together with preserving the material abrasion resistance.

Žarnovský a Kováč (2005) studied the wear of the excavator shovel teeth using surfacing by electrodes with a Cr content of up to 30 %. They reached the average values of the relative resistance to wear $\psi_{abr} = 1.2$ to 1.9.

Viňáš a Brezinová (2009) monitored the resistance to wear of the E 511B, E 518B and EW11 alkaline electrodes applied by GMAW to the tools of agricultural machines in operation (soil) and in laboratory conditions (corundum and grit stone). Surfacing welds were of one or of two layers, and the results obtained have confirmed the suitability of the selected method for the renovation of functional surfaces resisting abrasive wear.

Conclusions

The abrasive environment is characterised by specific properties causing an intensive wear and therefore it decreases the lifetime of functional parts in agricultural machinery tools. One of the possibilities for avoiding that is to create a layer resistant to wear using different surfacing methods of the filler material with its specific characteristics. We can say that the seedbed cultivator share location and the method of surfacing have a great impact on the wear extent. The method based on the principle of active gases is more effective in view of the surfacing method and the share lifetime.

Surfacing by the MIG and MAG methods can have many applications in operation due to their technical and economic advantages (expenses, operation), for example as compared to the laser surfacing with metal powders.

Súhrn

V príspevku sa zaoberáme posúdením vplyvu ochrannej atmosféry pri naváraní radličiek kompaktora proti abrazívnemu opotrebeniu. Pri stanovení odolnosti materiálu sme sledovali veľkosť opotrebenia na základe hmotnostných a lineárnych rozmerov. Kritérium oteruvzdornosti je pomerná odolnosť proti abrazívnemu opotrebeniu a tvrdosť HV 30 jednotlivých návarov na radličkách kompaktora. Dosiahnuté výsledky naznačili vhodnosť použitia ochranných plynov (zvlášť aktívnych, MAG) za účelom zvýšenia oteruvzdornosti a tým predĺženia životnosti radličiek kompaktora.